PEOPLE'S DEMOCRATIC REPUBLIC OF ALGERIA

MINISTRY OF HIGHER EDUCATION AND SCIENTIFIC

RESEARCH LAARBI TEBESSI UNIVERSITY OF

TEBESSA

FACULTY OF SCIENCE AND TECHNOLOGY

DEPARTMENT OF ELECTRICAL ENGINEERING

Master's Thesis

Specialty: Automatic and systems

Proportional resonant control design for voltage regulation of photovoltaic modules, enhancing the classical Perturb and Observe (P&O) method.

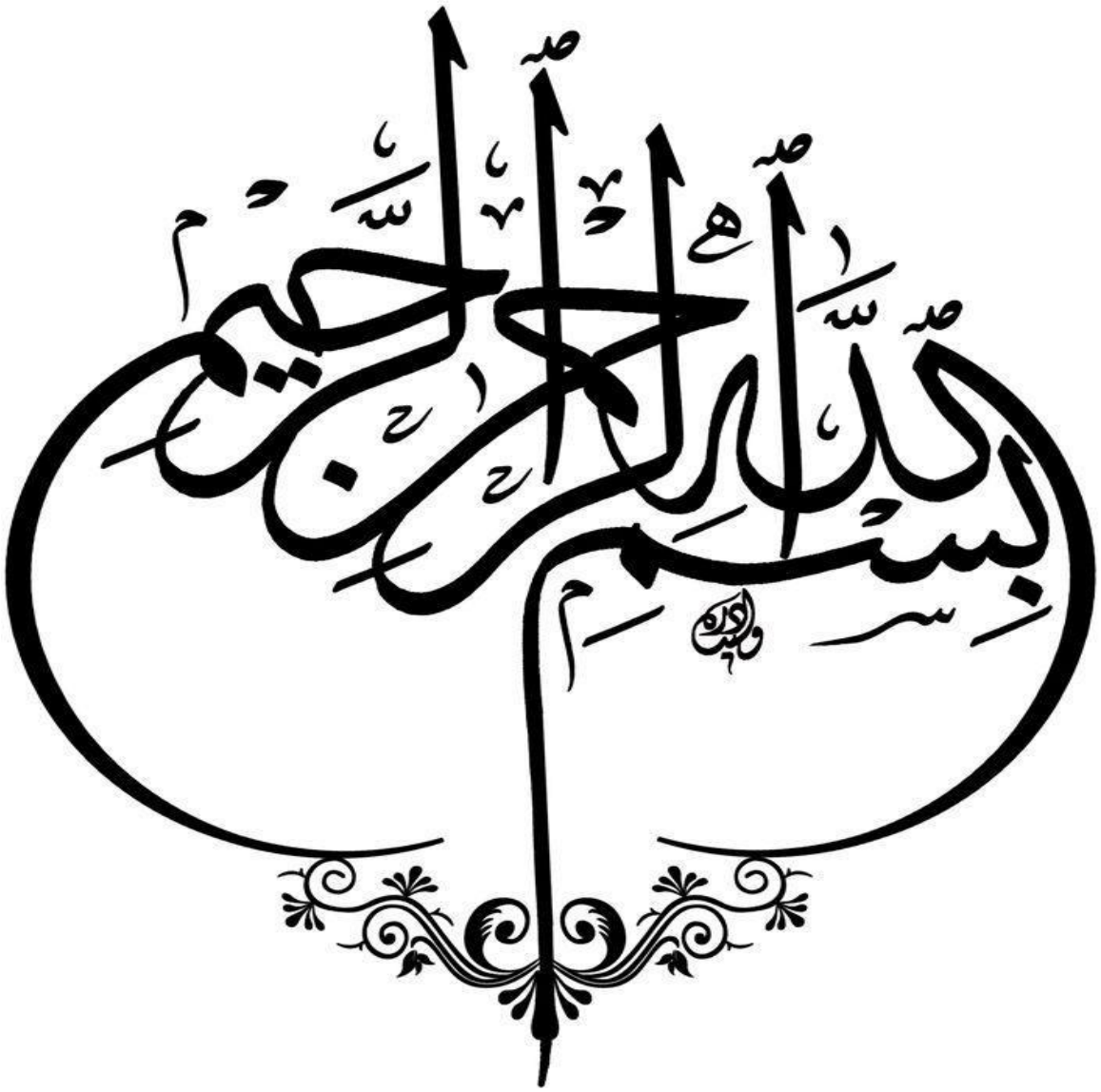
Presented by:

KHELIF Tarek & MERAHI Chaima

Members of jury:

President:	Dr. Laatra Yousfi
Supervisor:	Dr. Abdelhamid Djari
Examiner:	Dr. Riadh Djabri

University season: 2024/2025



»يَرْفَعِ ا هللاَّ ُلهذِينَ آمَنُوا مِنكُمْ وَالهذِينَ أُوتُوا الْعِلْمَ دَرَجَات«

المجادلة – الآية 11

ACKNOWLEDGEMENTS

First and foremost, we praise and thank Almighty God for His guidance and for granting us the strength, courage, health, and resources necessary to successfully complete this modest work.

We extend our sincere gratitude and appreciation to our dear and respected supervisor, Dr. **Abdelhamid Djari**, for his dedicated efforts, continuous support, constant presence, and valuable contributions throughout this sensitive period, which greatly facilitated the completion of this project.

We also express our profound thanks and appreciation to the members of the examination committee, Mr. **.....** and Mr ....., for their keen interest in our research, their gracious acceptance to evaluate our work, and their constructive comments and suggestions that enriched it.

Finally, we would like to sincerely thank everyone who contributed, directly or indirectly, to the realization of this project, praying that God rewards them abundantly for their efforts.

Dedication

Dedication

We, the undersigned, dedicate this modest work to:

Our dear parents, in recognition of their unwavering support, boundless sacrifices, and constant encouragement throughout our academic journey. Their dedication to our education and well-being has been a cornerstone of our success.

Our siblings, who have been a continuous source of inspiration and strength, offering love and motivation at every step.

Our friends and colleagues, whose companionship and assistance have been invaluable, sharing both challenges and triumphs along the way.

All those who, directly or indirectly, contributed to the completion of this work, whether through kind words, advice, or moral support.

Finally, we dedicate this work to ourselves, acknowledging the perseverance and determination that led us to overcome obstacles and achieve this goal.

Dedication

To the two women I proudly call Mom,

One who gave me life, and one who raised me with a heart full of love —

Your strength, your sacrifices, and your prayers have shaped the person I am today.

To the one who is unwell, I pray for your healing every day. May God grant you health and peace, for you deserve the world.

To my father — my role model and steady support,

Your quiet strength and endless encouragement have been my foundation.

Thank you for believing in me, even when I doubted myself.

To my sisters — my forever friends,

Your laughter, love, and unwavering presence have been my light on the darkest days.

I'm so grateful for every shared moment.

And to my only brother —

You've been my protector, my companion, and my strength.

Your support means more to me than words can express.

This achievement is not mine alone — it belongs to all of you.

Thank you for walking beside me on this journey.

I carry your love with me, today and always.

With all my heart,

[MERAHI Chaima]

Dedication

To my beloved parents, whose unconditional love, endless prayers, and unwavering belief in my abilities have been my foundation. Your sacrifices, guidance, and moral support have shaped who I am today, and I will forever be indebted to you.

Thank you for always standing by me in times of doubt and for constantly pushing me to strive for excellence.

To my brothers and sisters, thank you for being my pillars of strength. Your words of encouragement and your constant support have meant the world to me. Each one of you has, in your own unique way, contributed to my growth and success.

To my dear friends, especially those who accompanied me throughout this academic journey, thank you for the shared struggles, the moments of laughter, and the motivation to keep going even during the most challenging times.

Your companionship made this experience more meaningful and unforgettable.

To my respected teachers and supervisors, thank you for your invaluable knowledge, guidance, and mentorship. Your insights and feedback have played a critical role in shaping this work and in helping me evolve both intellectually and personally.

And finally, I dedicate this thesis to myself – for the countless sleepless nights, the perseverance, and the dedication it took to complete this chapter of my life.

This achievement stands as a testament to the power of resilience and hard work.

With all my heart, thank you.

[khelif Tarek]

CONTENTS

Summary

TABLE OF CONTENTS

List of figures	
List of tables	
List of symbols	
List of abbreviations	
Abstract	
General Introduction	1
Chapter I: Modeling of Photovoltaic Modules	
I.1. INTRODUCTION	5
I.2. MATHEMATICAL MODEL OF PV CELL	5
I.3. Current-voltage and power voltage characteristics	9
a. I-V Characteristic Curve	10
b. P-V Characteristic Curve	10
Ⅰ.4. Influence of Temperature on Photovoltaic Cells	11
4.1.Short-Circuit Current (Is_r^c)	11
4.2.Open-Circuit Voltage (V_o^c)	11
4.3. Maximum Power Output (P_max)	11
Ⅰ.5. Influence of Irradiation on Photovoltaic Cells	13
Ⅰ.6.DC-DC BOOST CONVERTER:	15
6.1. Boost Converter and its Operation	16
a. Switch Opened (Off State)	16
b. Switch Closed (On State)	17
c. Constant Output Voltage	18
Ⅰ.7. BUCK-BOOST CONVERTER BASICS	20
a. +Vin, -Vout (Negative Output) Configuration	21
b. +Vin, +Vout (Positive Output) Configuration	21
Ⅰ.8. CONCLUSION	23
Chapter 2: Synthesis of Direct/Indirect MPPT Control Using the P&O Algorithm	
Ⅱ. 1.Introduction	25
Ⅱ.2. direct connection between a PV generator and the charge	25
Ⅱ.3.System Modeling	27
Ⅱ. 4.Search for the maximum power point	28
Ⅱ.5.Principle of MPTT control	28
Ⅱ.6. Evaluation Criteria for an MPPT Controller	29
Ⅱ.7. MPPT Classification	30

Summary

7.1.Classification of MPPT Controls Based on Converter Parameters	31
7.1.1. MPPT Control Based on the Input Parameters of the Converter	31
7.1.2. MPPT Control Based on the Output Parameters of the Converter	31
7.2. Classification of MPPT Control Based on the Type of Search	32
7.2.1. Indirect Methods	32
7.2.2. direct Methods	32
Ⅱ.8. Maximum power point search technique	33
Ⅱ.9. Perturb & Observe (P&O)	33
Ⅱ.10.Conclusion	37
Chapter 3: Application of Proportional Resonant Control for Photovoltaic Module Voltage Regulation	
Ⅲ.1.Introduction	39
Ⅲ.2.PROPORTIONAL RESONANT CONTROLLER	39
A. PI Controller	39
B. PR controller	40
Ⅲ.3. Characteristics of the PR controllers	41
3.1. Perfect Tracking of Sinusoidal Signals (Zero Steady-State Error)	41
3.2.Disturbance Rejection at Specific Frequencies	41
3.3.High Selectivity with Minimal Impact on Other Frequencies	42
3.4.Suitability for AC Systems and Power Electronics	42
3.5.Simple Implementation in Stationary Reference Frame	42
Ⅲ.4. Proposed Controller	43
Ⅲ.5. Criterion for Evaluating MPPT Performance in PVG	45
a) efficiency criterion b) Energy consumption criterion	45 45

Summary

Ⅲ.6. Simulation Results	46
Ⅲ.7. Results Discussion	55
7.1 Output Power and Energy Efficiency	55
7.2 Duty Cycle Behavior	55
7.3 PV Voltage and Current Regulation	56
7.4 Control Signal Energy Consumption	56
Ⅲ.8. Conclusion	57

List of figures

List of figures

Figure No.	Title	Page
I.1	The configuration Of GCPV system.	7
I.2	PV module equivalent circuit	8
I.3	I-V and P-V characteristic curve of PV array simulation	9
I.4	Simulated I-V curve of PV module influenced by Temperature.	12
I.5	Simulated P-V curve of PV module influenced by Temperature	12
I.6	Simulated I-V and P-V curve of PV module influenced by solar illumination.	14
I.7	Basic boost converter circuit diagram	15
I.8	Transmission state of semiconductor switch.	16
I.9	The OFF-state diagram of the boost Converter When the switch is off, the sum total of inductor voltage and input voltage appear as the load voltage	17
I.10	The ON state diagram of the boost converter.	18
I.11	Inductor voltage waveform	19
1.12	Inductor current waveform	19
I.13	DC/DC Buck-Converter (negative type)	21
I.14	DC/DC Buck-Converter (Positive type)	22
II.1	Principle of Direct Coupling	25
II.2	Types of Loads in Direct Connection	26
II.3	PV Generator-Load Adaptation Stage	27
II.4	Diagram of a photovoltaic system with MPPT control	27
II.5	The P-V, I-V characteristic	28
II.6	Solar Energy conversion chain	29

List of figures

II.7	Principle of Impedance Matching via MPPT a) Using Input Parameters b) Using Output Parameters	31
II.8	Tracking the (MPP) using the Perturb and Observe (P&O) method	34
II.9	Flowchart of P&O method	35
III.1	PR controller	44
III.2	Resonant controller schemes	44
III.3	Synoptic diagram of the control loops	46
III.4	Block diagram of the P&O and PR controllers	46
III.5	The duty cycle of PV module with P&O and P&O_PR	47
III.6	Zoom of the duty cycle of PV module with P&O and P&O_PR.	47
III.7	The power of PV module with P&O and P&O_PR	48
III.8	Zoom at the power of PV module with P&O and P&O_PR	48
III.9	The Voltage of PV module with P&O and P&O_PR	49
III.10	Zoom at the Voltage of PV module with P&O and P&O_PR	49
III.11	The Current of PV module with P&O and P&O_PR	50
III.12	Zoom at the Current of PV module with P&O and P&O_PR	50
III.13	The duty cycle of PV module with P&O and P&O_PR	51
III.14	Zoom at the duty cycle of PV module with P&O and P&O_PR	51
III.15	The power of PV module with P&O and P&O_PR	52
III.16	Zoom at the power of PV module with P&O and P&O_PR	52
III.17	The duty cycle of PV module with P&O and P&O_PR	53

List of figures

III.18	Zoom at the duty cycle of PV module with P&O and P&O_PR	53
III.19	The Power of PV module with P&O and P&O_PR	54
III.20	Zoom at the Power of PV module with P&O and P&O_PR	54

List of tables

List of tables

Table No.	Title	Page
I.1	The PV module characteristics at (25 C° and 1000 W/ /m2)	9
II.1	Comparison of P&O and INC MPPT Techniques	37
III.1	Summary Table: PR Controller Objectives	42
III.2	Comparative Performance	56

List of symbols

List of symbols

List of symbols

symbol	Signification	unit
I	Electric current (Pv output or system)	Ampere(A)
V	Voltage	Volt(V)
P	Power	Watt(W)
Iph	Photocurrent (light-generated)	Ampere(A)
Is	Diode sturation	Ampere(A)
Id	Diode current	Ampere(A)
V_T	Thermal voltage	Volt(V)
Rsh	Shunt resistance	Ohm(Ω)
n	Ideality factor	Dimensionless
k	Boltzmann constant ($1.38*10^{-23}$)	J/k
T	Temperature	Kelvin(k)
q	Electron charge ($1.6*10^{-19}$	Coulomb(C)
V_{mpp}	Voltage at maximum power point	Volt(V)
I_{mpp}	Current at maximum power point	Ampere (A)
G=I/V	Conductance	Siemens(S)
$\frac{dI}{dV}$	Derivative of current with respect to voltage	A/V
$\frac{dP}{dV}$	Derivative of power with respect to voltage	W/V
P_{old}	Previous power(before change)	Watt(W)
D	Duty cycle	Dimensionless
f	Switching frequency	Hertz (Hz)
ΔI_L	Inductor current ripple	Ampere(A)
ΔV_0	Output voltage	Volt (V)

List of symbols

R_0	Output load resistance	Ohm(Ω)
Iopt	Optimal current (at MPP)	Ampere(A)
Vopt	Optimal voltage (at MPP)	Volt(V)
Impp	Current at Maximum Power Point	Ampere(A)
Pnew	Power after recent perturbation	Watt(W)
Pold	Previously measured power	Watt(W)
E	Error in power change (used in Fuzzy Logic MPPT)	Watt(W)

List of abbreviation

List of abbreviation

Abbreviation	Full Term
PV	Photovoltaic
GCPV	Grid-Connected Photovoltaic
MPPT	Maximum Power Point Tracking
I-V	Current-Voltage
P-V	Power-Voltage
Voc	Open-Circuit Voltage
I_{sc}	Short-Circuit Current
Pmax	Maximum Power
Vmp	Voltage at Maximum Power
Imp	Current at Maximum Power
I_{ph}	Photocurrent
Id	Diode Current
Is	Diode Saturation Current
VT	Thermal Voltage
R_{se}	Series Resistance
R_{sh}	Shunt Resistance
DC	Direct Current
AC	Alternating Current
Vg	Input Voltage (DC source)
L	Inductance
C	Capacitance
D	Diode (or Duty Cycle, depending on context)
R	Resistance

List of abbreviation

CCM	Continuous Conduction Mode
Vin	Input Voltage
V_{out}	Output Voltage
dq-frame	Direct-Quadrature Frame (used in inverter control)
T	Switching Period
G(s)	Transfer Function in Laplace Domain
MPP	Maximum Power point
GPV	Photovoltaic Generator
P&O	Perturb and Observe
INC	Incremental Conductance
ANN	Artificial Neural Networks
PWM	Pulse Width Modulation
PI	Proportional-Integral
PR	Proportional Resonant
Ef	Efficiency
IACS	Integral Absolute Control Signal
αβ	Alpha-Beta Frame
dq	Direct-Quadrature Frame
UPS	Uninterruptible Power Supply
SOGI	Second-Order Generalized Integrator

Abstract

Abstract

As the world increasingly turns to renewable energy to combat climate change and reduce dependence on fossil fuels, photovoltaic (PV) systems have become a cornerstone of sustainable energy solutions. Their performance, however, relies heavily on control strategies that maximize energy extraction and ensure stability under varying environmental conditions. One of the most commonly used techniques for maximum power point tracking (MPPT) is the Perturb and Observe (P&O) algorithm. While simple and widely adopted, the P&O method suffers from drawbacks such as power oscillations, slow dynamic response, and poor performance under rapidly changing irradiance. This thesis aims to overcome these limitations by enhancing the classical P&O algorithm with a Proportional Resonant (PR) controller, known for its accuracy and selective frequency amplification. By integrating the PR controller into the voltage regulation loop, the proposed method improves dynamic response, reduces steady-state oscillations, and ensures more stable and efficient power delivery. The work is structured into three chapters: the first focuses on modeling PV modules; the second analyzes the classical P&O method in both direct and indirect control configurations; and the third presents the implementation of the improved P&O + PR control strategy. Simulation results confirm that the proposed approach significantly outperforms the traditional P&O algorithm, making it a promising solution for real-world PV applications.

Abstract

ملخص

مع التوجه المتزايد للعالم نحو الطاقة المتجددة لمواجهة التغير المناخي وتقليل الاعتماد على الوقود الأحفوري، أصبحت الأنظمة الكهروضوئية (PV) حجر الأساس في حلول الطاقة المستدامة. إلا أن أداء هذه الأنظمة يعتمد بشكل كبير على استراتيجيات التحكم التي تهدف إلى تعظيم استخلاص الطاقة وضمان الاستقرار تحت ظروف بيئية متغيرة. تُعتبر خوارزمية "الاضطراب والملاحظة " (Perturb and Observe - P&O)من أكثر التقنيات استخداماً لتتبع نقطة القدرة العظمى(MPPT) ، ورغم بساطتها وسهولة تنفيذها، إلا أنها تعاني من بعض العيوب مثل التذبذب حول نقطة القدرة العظمى، الاستجابة الديناميكية البطيئة، والأداء الضعيف في ظل التغيرات السريعة في الإشعاع الشمسي .تهدف هذه الرسالة إلى معالجة هذه العيوب من خلال تحسين الخوارزمية الكلاسيكية

P&Oباستخدام متحكم تناسبي-رنين(Proportional Resonant - PR) ، والذي يتميز بدقته وقدرته على تضخيم الترددات

المطلوبة بشكل انتقائي. من خلال دمج هذا المتحكم في حلقة تنظيم الجهد، تُحسن الطريقة المقترحة من الاستجابة الديناميكية، وتُقلل التذبذبات في الحالة المستقرة، وتُوفر قدرة أكثر استقرارًا وكفاءة .تتكون هذه الرسالة من ثلاثة فصول: يركّز الفصل الأول على نمذجة الوحدات الكهروضوئية، بينما يعرض الفصل الثاني تحليلًا لخوارزمية P&O الكلاسيكية باستخدام التحكم المباشر وغير المباشر. أما الفصل الثالث، فيتناول تنفيذ استراتيجية التحكم المُحسّنة .P&O + PR وتُظهر نتائج المحاكاة أن النهج المقترح يتفوق بشكل ملحوظ على الخوارزمية التقليدية، مما يجعله حلًا واعدًا لتطبيقات الطاقة الكهروضوئية الواقعية.

Abstract

Résumé

À mesure que le monde se tourne de plus en plus vers les énergies renouvelables pour lutter contre le changement climatique et réduire la dépendance aux combustibles fossiles, les systèmes photovoltaïques (PV) s'imposent comme une pierre angulaire des solutions énergétiques durables. Toutefois, leurs performances dépendent fortement des stratégies de commande mises en œuvre, qui visent à maximiser l'extraction de l'énergie et à assurer une stabilité optimale sous des conditions environnementales variables. Parmi les techniques les plus utilisées pour le suivi du point de puissance maximale (MPPT), l'algorithme Perturb and Observe (P&O) se distingue par sa simplicité et sa facilité d'implémentation. Néanmoins, il présente des inconvénients notables, tels que des oscillations autour du point de puissance maximale, une réponse dynamique lente et une faible efficacité en cas de variations rapides de l'irradiance. Ce mémoire propose de surmonter ces limitations en améliorant l'algorithme classique P&O grâce à l'intégration d'un régulateur résonant proportionnel (PR), reconnu pour sa précision et sa capacité à amplifier sélectivement certaines fréquences. En l'intégrant dans la boucle de régulation de tension, cette méthode permet d'améliorer la réponse dynamique, de réduire les oscillations en régime permanent et de garantir une production d'énergie plus stable et plus efficace. Le travail est structuré en trois chapitres : le premier est consacré à la modélisation des modules photovoltaïques ; le second analyse l'algorithme P&O classique selon les approches de commande directe et indirecte ; enfin, le troisième présente l'implémentation de la stratégie de commande améliorée combinant P&O et PR. Les résultats de simulation démontrent que la méthode proposée surpasse largement l'approche classique, ce qui en fait une solution prometteuse pour les applications photovoltaïques en conditions réelles.

General introduction

General Introduction

The increasing global demand for renewable energy, driven by environmental concerns and the depletion of fossil fuels, has placed photovoltaic (PV) energy at the forefront of sustainable energy solutions. Photovoltaic systems, which directly convert solar energy into electricity, have become essential components of smart energy grids, distributed generation systems, and standalone power units. However, the efficiency and reliability of PV systems depend heavily on their control strategies, which ensure optimal power extraction and stable operation under variable environmental conditions.

One of the most common and widely used methods for extracting the maximum power from PV modules is the **Perturb and Observe (P&O)** algorithm. Despite its simplicity and ease of implementation, the P&O method suffers from oscillations around the Maximum Power Point (MPP), slow dynamic response, and sensitivity to rapid irradiance variations. These limitations affect both the efficiency and the long-term reliability of PV systems, especially in dynamic or partially shaded environments.

To address these challenges, this thesis proposes an improved control strategy that enhances the classical P&O method by integrating a **Proportional Resonant (PR) controller** into the voltage regulation loop. The PR controller is well known for its ability to eliminate steady-state error for sinusoidal signals and improve system robustness by selectively amplifying the fundamental frequency component while attenuating high-frequency noise and disturbances. By embedding the PR controller into the control structure, the PV system benefits from improved dynamic response, reduced oscillations, and more stable power delivery.

This thesis is organized into three chapters:

- **Chapter 1: Modeling of Photovoltaic Modules**

  This chapter presents the electrical modeling of PV cells and modules. It introduces the single-diode and double-diode models and explains the relationship between irradiance, temperature, voltage, and current. A detailed simulation of the PV module is developed to serve as a test platform for evaluating the proposed control strategies.

- **Chapter 2: Synthesis of Direct/Indirect MPPT Control Using the P&O Algorithm**
  In this chapter, the classical P&O MPPT technique is implemented and analyzed. Both direct and indirect control approaches are discussed in the context of DC-DC converters. The performance of the basic P&O algorithm is evaluated under various operating conditions, highlighting its limitations in dynamic scenarios and justifying the need for improved control.
- **Chapter 3: Application of Proportional Resonant Control for Photovoltaic Module Voltage Regulation**
  The core contribution of this thesis lies in this chapter, where a Proportional Resonant (PR) controller is designed and integrated with the P&O algorithm. The PR controller regulates the PV module voltage with high precision, enhancing the MPPT performance. Through simulations, the combined approach (P&O + PR) is evaluated and compared with the classical P&O method.

Chaptre I:

Modeling of Photovoltaic modules

I.1. INTRODUCTION

Energy is essential for human life and the economy, and with the industrial revolution, global energy demand has significantly increased. In recent years, concerns about the energy crisis have grown. As a result, Photovoltaic (PV) systems have gained attention as one of the most promising renewable energy sources. PV solar generation is favored due to its advantages, such as no fuel costs, environmental benefits, low maintenance, and silent operation. However, high installation costs and low energy conversion efficiency are key challenges for PV systems [1].

To optimize energy output and improve efficiency, power electronics conversion circuits are needed. DC-DC converters are crucial in enhancing the performance of renewable energy sources. Since photovoltaic and fuel cells provide low voltage, which is insufficient for inverters, high-voltage gain, high-efficiency DC-DC converters are preferred. These converters reduce both costs and system size [2].

A key type of DC-DC converter is the Buck-Boost converter, which can either step up or step-down voltage. This is particularly useful for PV systems, where input voltage fluctuates with changes in sunlight. The Buck-Boost converter ensures efficient and stable operation by adjusting voltage to the required level, making it a vital component in enhancing the performance of PV systems.

I.2. MATHEMATICAL MODEL OF PV CELL

The general mathematical description of the I-V output characteristics for a photovoltaic (PV) cell has been studied for over the past four decades. This equivalent circuit-based model is primarily used in Maximum Power Point Tracking (MPPT) technologies [1].

The equivalent circuit of the general model Fig.2. which includes:

- **Photocurrent (Iph):** This is the current generated by the solar cell due to sunlight. It is directly proportional to the intensity of the light incident on the cell.
- **Diode (D):** In the equivalent circuit, the diode represents the key component that models the behavior of the P-N junction of the solar cell.

- ✓ The diode blocks current when a small reverse voltage is applied, representing the behavior of the solar cell in dark or low-light conditions.

- ✓ Under illumination, the diode allows the photocurrent to flow in the correct direction and significantly influences the I-V relationship of the solar cell.

- **Diode Saturation Current (Is):** This is the current that flows through the diode in the dark (i.e., without light). It is a key factor in determining the overall current- voltage behavior of the cell.
- **Iᴅ (Diode Current)**

- ✓ Iᴅ represents the current passing through the diode when the solar cell is operating under both light and dark conditions.
- ✓ The diode current (Iᴅ) is calculated using the Shockley diode equation, which is a function of the voltage across the diode and its reverse saturation current Is. The general form of this equation is:

$$I_D = I[e^{\frac{V}{\propto VT}} - 1] \qquad (1)$$

- **Series Resistance (Rse):** This represents the internal resistance of the solar cell, which arises from factors like the resistance of the semiconductor material, contacts, and interconnections. It leads to power loss when current flows through the cell.
- **Shunt Resistance (Rsh):** This represents leakage current paths that bypass the diode. It models the effect of any leakage current that might flow across the solar cell, reducing the overall efficiency.

The voltage-current characteristic equation of a solar cell is expressed as [1]:

$$I = [\frac{I_{Ph} - I_S}{e^{\frac{V \pm I*Rse}{\propto VT}} - 1}] - \frac{V + I*Rse}{Rsh} \qquad (2)$$

$$VT = n\frac{KT}{q} \quad (3)$$

Where:

- **I:** is the output current (A).
- **V:** is the output voltage across the solar cell(V).
- **Iph:** is the photocurrent (light-generated current) (A).
- **Is:** is the diode saturation current (A).
- **A:** is the ideality factor (typically between 1 and 2).
- **Rse:** is the series resistance of the cell (Ohm).
- **Rsh:** is the shunt resistance of the cell (Ohm).
- **VT:** is the thermal voltage.

Thermal Voltage (VT): Given by the equation (3), where:

- **n:** is the ideality factor (typically between 1 and 2).
- **K:** is the Boltzmann constant (1.38×10^{-23} J/K).
- **T:** is the temperature of the cell (in Kelvin).
- **q:** is the charge of an electron (1.6×10^{-19} C). The thermal voltage varies with temperature and is typically around 0.025V at room temperature.

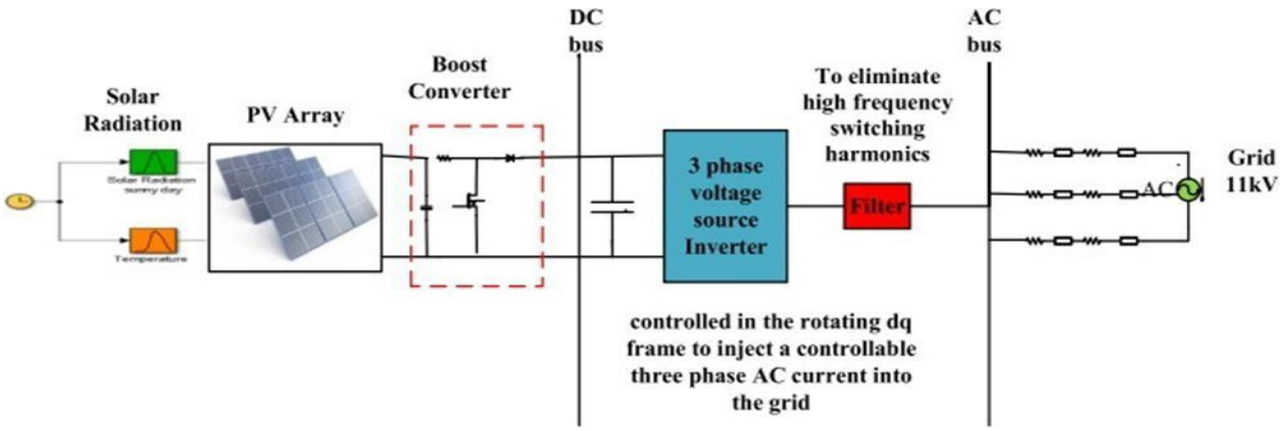


Fig I.1. The configuration Of GCPV system.

The system shown generates electricity from solar energy and feeds it into the power grid at 11 kV. The process starts with the photovoltaic (PV) array, which converts sunlight into DC electricity based on solar irradiance and temperature. The voltage is then increased by a boost converter using MPPT technology to optimize power extraction. The DC electricity is sent to a three-phase inverter, which converts it into AC, synchronized with the grid using dq- frame control. Harmonics from the inverter are filtered out to ensure high-quality AC power. The clean AC is fed into the grid, with excess energy exported or drawn from the grid as needed. This setup is part of a grid-connected PV system (GCPV).

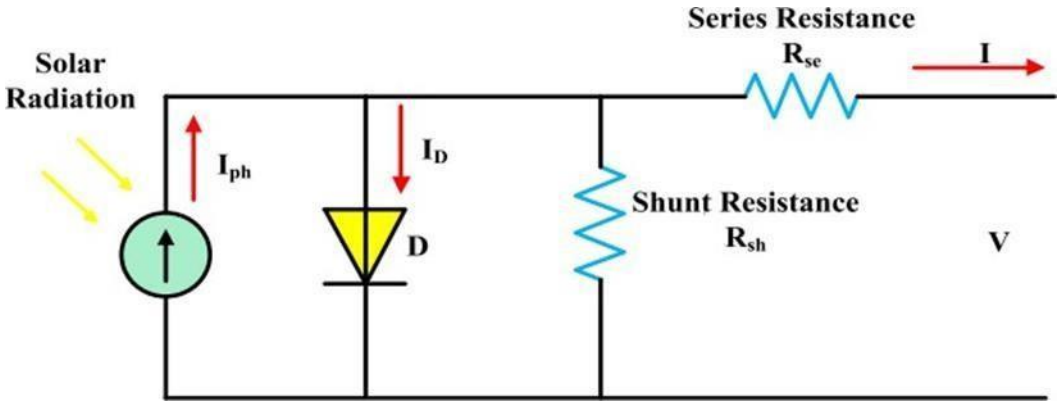


Fig I.2. PV module equivalent circuit

The image shows the equivalent circuit of a PV cell, which converts solar energy into electrical energy. Photons from sunlight excite electrons in the semiconductor (e.g., silicon), generating a photocurrent (Iph). The diode in the circuit represents the reverse current (ID) due to the semiconductor's properties, which increases with temperature. The circuit includes series resistance (Rse), representing energy losses, and shunt resistance (Rsh), indicating leakage currents. To maximize efficiency, Rse should be minimized, and Rsh should be maximized. The generated DC current passes through the series resistance and is collected from interconnected cells in the PV array to power the inverter.

Parameter	Value
Maximum power	60 W
Tension at Pmax	17.1 V
Current at Pmax	3, 5 A
Open circuit voltage	21.1 V
Short circuit current	3.8 A

Table I.1: The PV module characteristics at (25 C° and 1000 W/ /m2)

Table 1 presents the electrical characteristics of the photovoltaic (PV) module at a temperature of 25°C and a solar irradiance of 1000 W/m². From the data, it can be observed that the maximum power output of the module is 60 W, which occurs at a voltage of 17.1 V and a current of 3.5 A. The table also shows that the open circuit voltage is 21.1 V, while the short circuit current is 3.8 A. These parameters are essential for determining the optimal operating point of the PV module and achieving high efficiency in solar energy utilization.

I.3. Current-voltage and power voltage characteristics

One way of studying the consistency of the model is developed to study the shape of the current-voltage characteristics I(V), (Fig I.3) and P(V), power-voltage, was obtained using the equations the electrical model {eq. (02)}[1].

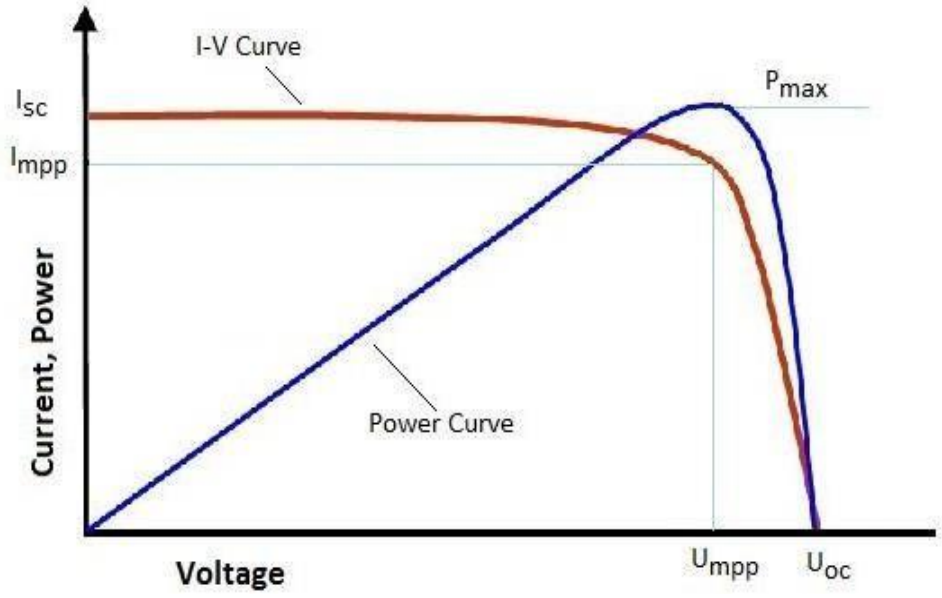


Fig I.3. I-V and P-V characteristic curve of PV array simulation [31].

The provided curves illustrate the current-voltage (I-V) and power-voltage (P-V) characteristics of the photovoltaic (PV) array. These curves help us understand the behavior and performance of the PV array in response to variations in voltage.

a) I-V Characteristic Curve

The I-V curve shows how the output current of the PV array varies with the output voltage. At the start, the current remains almost constant as the voltage increases, indicating that the PV array can provide a steady current regardless of slight voltage changes. This region corresponds to the operation under high irradiance conditions. However, as the voltage continues to rise and approaches the open-circuit voltage (Voc), the current rapidly drops to zero. This behavior reflects the fundamental characteristic of a PV cell: high current at low voltages and a sharp decline near Voc.

- **At very low voltages**, the current is very high because the solar cell is operating at its maximum short-circuit current (**Iph**), and the current is mainly governed by the photocurrent.
- **As the voltage increases**, the current starts to drop due to the diode's exponential behavior and the internal resistance.
- **At high voltages**, the current approaches zero, and the behavior of the curve is dominated by the reverse saturation current (**Is**) of the diode.

b) P-V Characteristic Curve

The P-V curve represents the relationship between the power output and the voltage of the PV array. As the voltage increases from zero, the power also increases, reaching its peak at a specific point known as the Maximum Power Point (MPP). At this point, the PV array delivers its maximum possible power, which is crucial for optimizing energy extraction. Beyond the MPP, if the voltage continues to increase, the power output decreases sharply, eventually reaching zero at the open-circuit voltage. The peak point on the P-V curve is where the MPPT (Maximum Power Point Tracking) controller operates to ensure the system always works at the maximum power level.

The P-V curve typically has a peak at a certain voltage, which represents the maximum power point (MPP). This point is crucial for the efficiency of the solar cell, as it is where the solar cell produces the maximum possible power.

I.4. Influence of Temperature on Photovoltaic Cells

When studying photovoltaic cells (PV), the one-diode model presented earlier is used to determine the voltage (V), current (I), and generated power (P). Temperature has a significant effect on the characteristics of the solar cell, including the current-voltage (I-V) curve and the power-voltage (P-V) curve (Fig .4) and (Fig .5) [1].

4.1. Short-Circuit Current (Is_r^c)

- As the **temperature** increases, **the short-circuit current (Is_r^c)** increases slightly. This increase is limited (approximately 0.1 A at 25°C).
- This happens because **the photocurrent (Iph),** which depends on solar irradiance, is affected by the increase in temperature. However, the increase in temperature leads to opposite effects on the voltage (as seen in the next point).

4.2. Open-Circuit Voltage (V_o^c)

- The **open-circuit voltage (V_o^c)** decreases as temperature increases.
- This decrease occurs because the **reverse saturation current (Is)** of the diode increases with temperature. As a result, the voltage across the diode becomes lower at higher temperatures.

4.3. Maximum Power Output (P_max)

- The increase in temperature also results in a **reduction in the maximum power output.**
- As temperature increases, the voltage (V) decreases more than the increase in current (I), leading to a decrease in **maximum power output (P_max).** This is due to the effects of temperature on the internal resistance of the cell (series and shunt resistances) and the impact on the diode's characteristics.

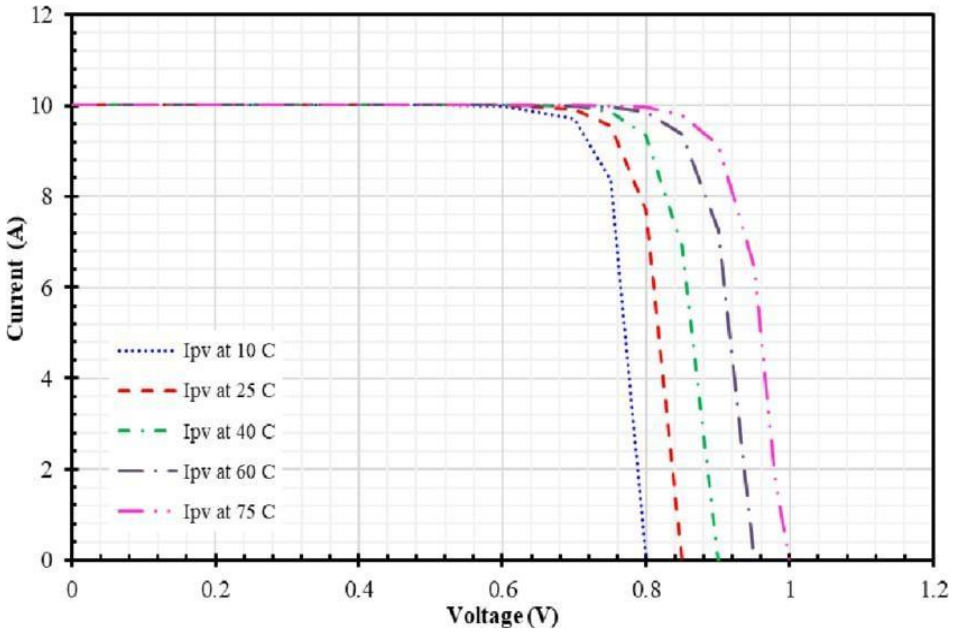


Fig I.4. Simulated I-V curve of PV module influenced by Temperature [32].

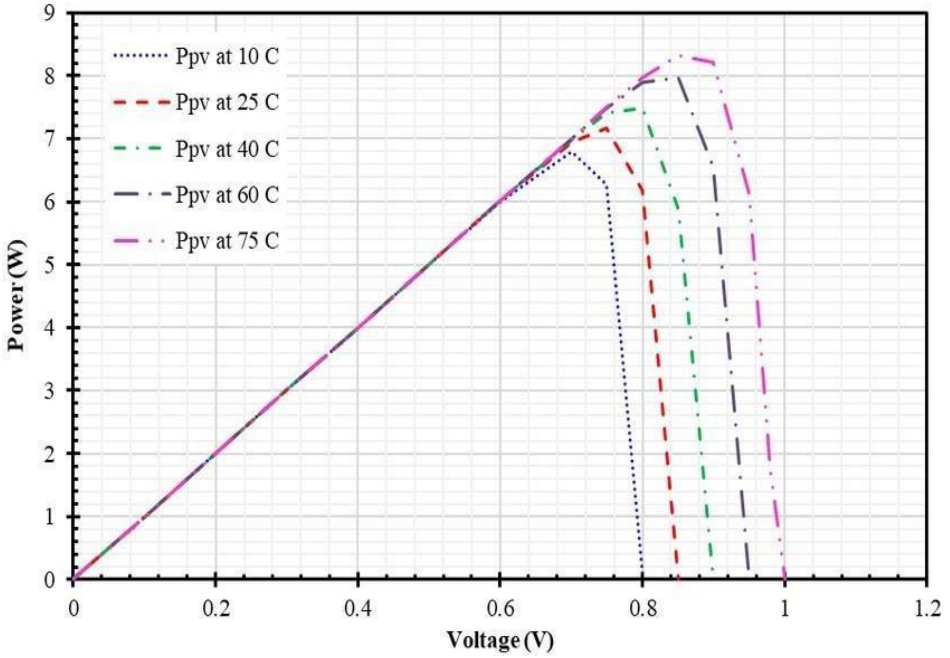


Fig I.5. Simulated P-V curve of PV module influenced by Temperature [32].

- The **I-V** curve and **P-V** curve for the Msx60 panel under a solar irradiance of 1000 W/m² are shown in **Fig 4** and **Fig 5** for different temperature values.
- From these curves, we can observe the changes that occur with increasing temperature
- As the temperature rises, there is a slight increase in short-circuit current (Is_r^c).
- The open-circuit voltage (V_o^c) decreases significantly.

- Maximum power output (P_max) decreases with an increase in temperature.

- **Physical Explanation**

As the temperature rises, the solar cell becomes less efficient in converting solar energy into electricity, as the excess heat leads to an increase in reverse current within the diode, reducing the voltage produced by the cell. The effect of the internal resistance of the cell (such as series resistance and shunt resistance) exacerbates this effect.

I.5. Influence of Irradiation on Photovoltaic Cells

The irradiation or solar illumination plays a critical role in the performance of photovoltaic (PV) cells, influencing both the current-voltage (I-V) and power-voltage (P-V) in Fig.6 characteristics [1].

- **As solar irradiance increases** (i.e., higher levels of sunlight), both the short-circuit **current (Is_r^c)** and open-circuit voltage (V_o^c) increase to some extent, resulting in a higher **maximum power output (P_max).**
- **At higher irradiation levels**, the **photocurrent (Iph)** generated by the solar cell increases, which directly increases the **short-circuit current.**
- However, **the open-circuit voltage (V_o^c)** doesn't increase as significantly, but it still shows an increase in response to higher solar illumination, as more p hotons are available to excite the electrons in the cell.

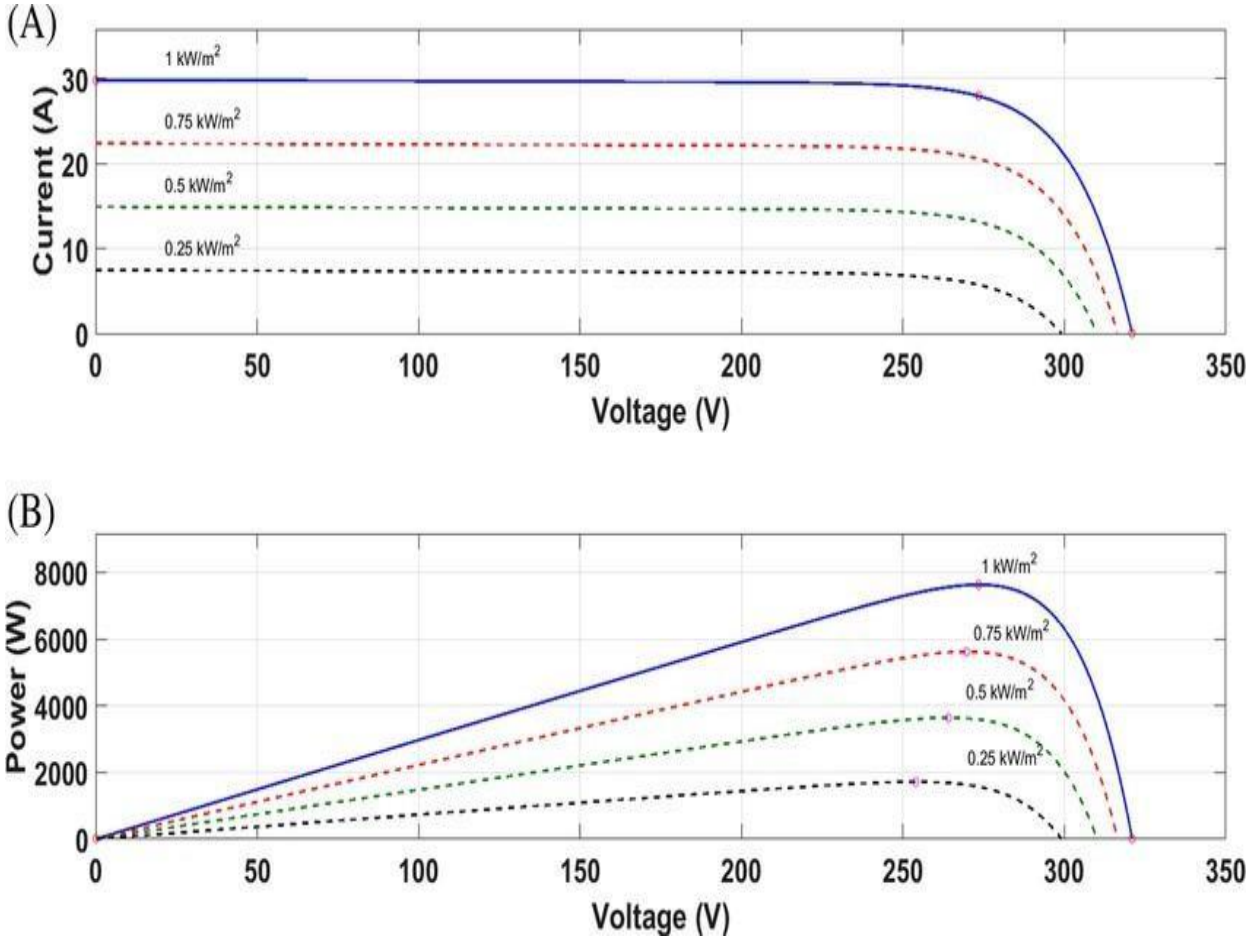


Fig I.6. Simulated I-V and P-V curve of PV module influenced by solar illumination [33].

Fig.6 shows:

- the **I-V curve** for the **Msx60 photovoltaic module** at a temperature of **T= 25°C** under various levels of solar irradiance.
    - As the irradiation increases, the **short-circuit current (Is_r^c)** increases, resulting in a higher current for the same voltage.
    - The **open-circuit voltage (V_o^c)** also increases slightly but not as much as the short-circuit current.
- the corresponding **P-V** curve for the same module at the same temperature and different illumination levels.
    - The **maximum power (P_max)** increases with higher solar illumination.

o At higher irradiance levels, the cell produces more power because of the increased photocurrent generated by the greater number of incident photons.

I.6. DC-DC BOOST CONVERTER

The boost converter is a system that transmits the output voltage to a higher voltage level by increasing the correct voltage at the input of the converter. Fig.9 shows the basic circuit form. As shown in Fig.9, the semiconductor switch consists of diodes, inductors and capacity elements. It consists of a DC input voltage source Vg, a boost inductor L, a controlled switch S, a diode D, a filter capacitor C, and a load resistance R. When the switch is transmitted S, the source voltage completes the circuit via the inductor and the switch. It stores some energy on the inductor. In this case, the diode is in reverse polarity and load of output feeds to the capacitor. The current of the capacitor is high. the current through the boost inductor increases linearly, and the diode D remains off during this time [2].

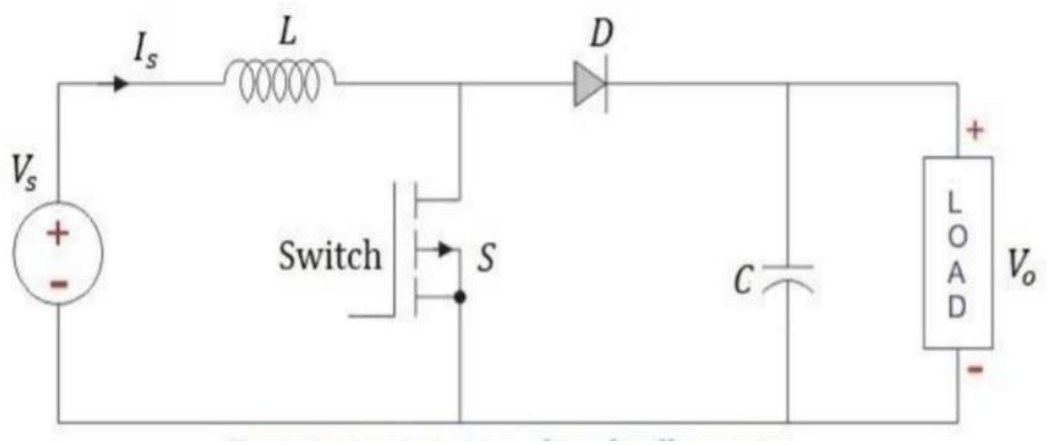


Fig I.7. Basic boost converter circuit diagram

- DC Input Voltage Source (Vg): This is the source that provides the initial voltage to the converter.
- Boost Inductor (L): The inductor stores energy when the switch is closed and releases it when the switch is open.
- Controlled Switch (S): Typically, a transistor or MOSFET, this switch controls the timing of energy storage and release.

- Diode (D): The diode prevents reverse current and ensures current flows in the proper direction when the switch is open.
- Filter Capacitor (C): This capacitor smooths the output voltage to remove ripples.
- Load Resistance (R): This is the load connected to the output of the boost converter.

Once the switch is turned off S, the current that was passing through the inductor begins to flow through the diode towards the capacitor and the load. The inductor releases its stored energy, and the polarity of the voltage across the inductor matches the polarity of the voltage source, connecting to the load through the diode. This results in an increase in the output voltage. At this point, the diode enters cutoff, and the circuit splits into two distinct parts, as shown in Fig.01. The output voltage remains stable as long as the time constant of the RC circuit is significantly greater than the switching period.

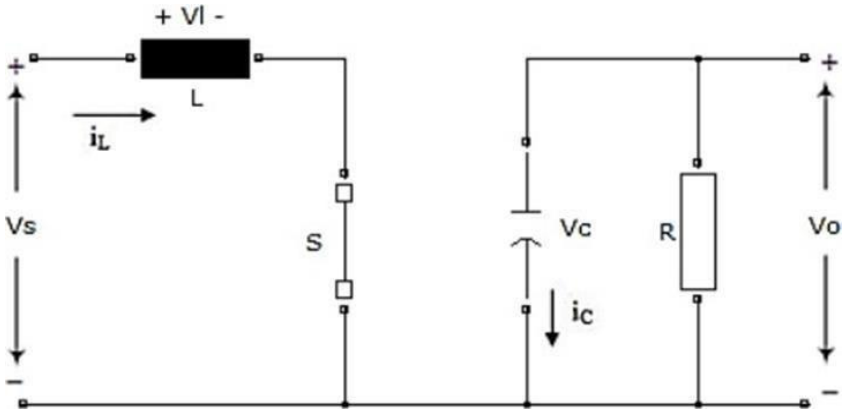


Fig I.8. Transmission state of semiconductor switch.

6.1. Boost Converter and its Operation

a) Switch Opened (Off State):

- As soon as the switch (S) is turned off, the energy stored in the inductor begins to release.
- The current flowing through the inductor now flows through the diode (D), charging the capacitor and supplying energy to the load.
- The polarity of the inductor voltage is the same as the voltage source, and the energy from the inductor increases the output voltage.
- The diode becomes forward biased and conducts current to the capacitor and the load.
- The energy stored in the inductor is released, and the output voltage is boosted.

In the OFF state, the circuit becomes as shown in the **Fig.9.**[3].

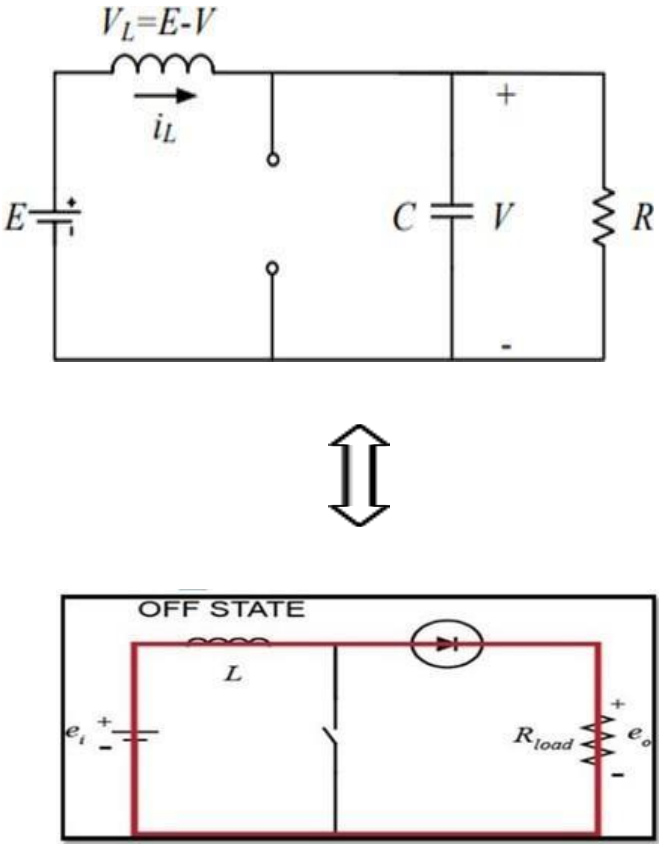


Fig I.9. The OFF-state diagram of the boost Converter When the switch is off, the sum total of inductor voltage and input voltage appear as the load voltage

b/ Switch Closed (On State)

- When the switch (S) is closed, the input voltage (Vg) completes the circuit through the inductor and the switch.
- Energy is stored in the inductor, and the current through the inductor increases linearly.
- During this time, the diode (D) is reverse biased (it does not conduct), and the output is fed to the capacitor. The capacitor current is high, and energy is stored in the capacitor.

In the ON state, the circuit diagram is as shown below in the Fig.12.[3].

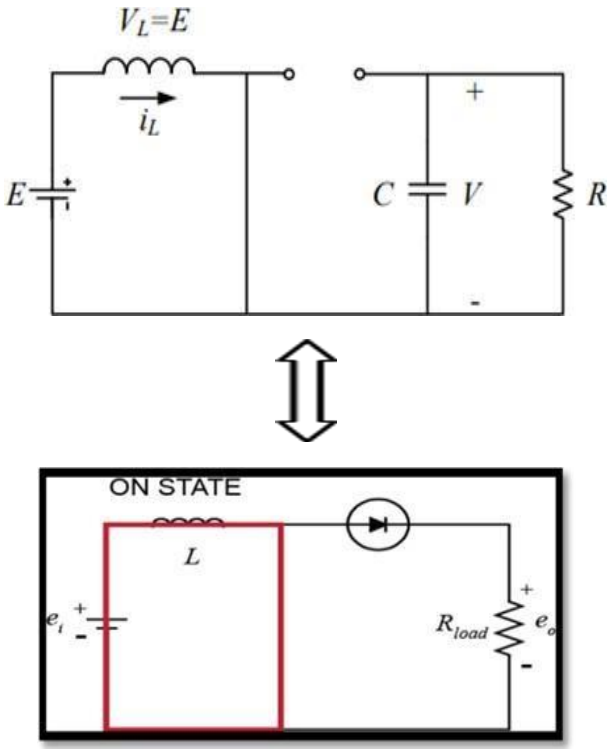


Fig I.10. The ON state diagram of the boost converter.

c) Constant Output Voltage

- As long as the time constant of the RC circuit (the filter capacitor and the load resistance) is much greater than the switching period, the output voltage remains constant and stable.
- The filter capacitor helps smooth out any voltage ripples, ensuring a steady output.

When the switch S is closed, the diode D is reverse biased and turns off. In this mode, the current through the inductor increases linearly, and the capacitor supplies power to the load. In the second mode, when the switch is turned off, the stored current in the inductor discharges through the diode to the load. Therefore, in this mode, both the inductor current and the capacitor voltage provide power to the load. The waveforms of the steady-state operation of the converter during one switching period are shown in Fig 00 et 01. From Fig 00 et 01, the voltage across the inductor L during a switching period T is [4]:

$$VL\,(t) = \{ \begin{matrix} E & during & DT \\ E - V & durin & 1 - D \end{matrix} \} \qquad (4)$$

Due to the volt-second balance, the average voltage across the inductor in one switching period must be zero then,

$E.DT + (E - V)(1 - D)T = 0$ (5)

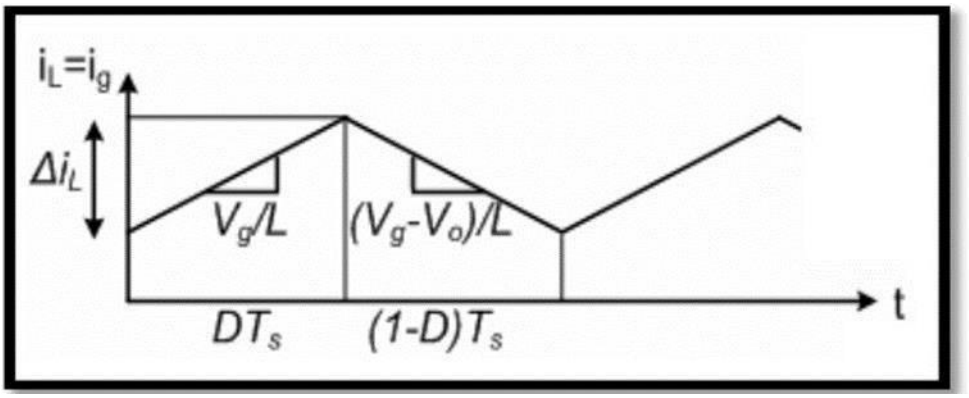


Fig I.11. Inductor voltage waveform

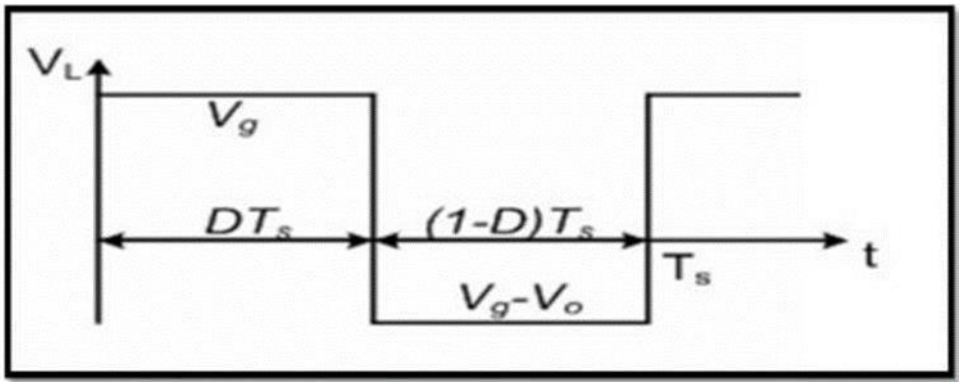


Fig I.12. Inductor current waveform

When the switch is ON, the inductor is charged from the input voltage source Vg and the capacitor discharges across1 the load. The duty cycle [3].

$$D = \frac{T_{ON}}{T} \quad (5)$$

Where: $$T = \frac{1}{f} \quad (6)$$

$Vg\ (DTs) + (Vg - V_o)(1 - D)\ Ts = 0$ (7)

$Vg\ (DTs) - Vg\ (DTs) - Vg\ Ts + V_o DTs - V_o Ts = 0$ (8)

$$V_0 = \frac{V_g}{1-D} \quad (9)$$

$$\frac{V_0}{V_g} = \frac{1}{1-D} \quad (10)$$

From Inductor current ripple analysis, change in inductor current,

$$\Delta IL = (Imax - Imin) \quad (11)$$

$$\Rightarrow \Delta IL = (Vg/L * (DTs)) \quad (12)$$

$$\Rightarrow \Delta IL = (VgD)/fsL \quad (13)$$

$$L = VgD/f(\Delta IL) \quad (14)$$

The boost converter operates in CCM (continuous conducting mode) L>Lb where

$$Lb = \frac{(1-D)2DR}{2f} \quad (15)$$

We have :

$$\frac{\Delta V0}{V0} = \frac{DTs}{R0C} \quad (16)$$

$$R0 = \frac{V0}{I0} \quad (17)$$

$$C = \frac{D}{f} * R0 * \left(\frac{\Delta V0}{V}\right) \quad (18)$$

$$(s) = \frac{V0}{1-V} * \frac{1-\frac{Ls}{(1-D)^2 * R}}{\frac{LCs^2}{(1-D)^2} + \frac{Ls}{(1-D)^2 * R}} \quad (19)$$

The transfer function of the boost converter used for the modeling is given by: Putting the values of R, L, C, D, Vg in the above equation.

I.7. BUCK-BOOST CONVERTER BASICS

The buck-boost DC-DC converter provides greater flexibility compared to the individual buck or boost converters. As expected, additional components may be needed to achieve the required functionality [1].

There are several configurations available for buck-boost converters:

a. +Vin, -Vout (Negative Output) Configuration:

- **Description**
  - In this configuration, the buck-boost converter produces a negative output voltage (Vout) from a positive input voltage (Vin).
  - It uses the same number of components as the simple buck or boost converters.
- **Operation**
  - When the switch is closed, the current builds up through the inductor.
  - When the switch is opened, the inductor supplies current through the diode to the load.
  - The polarities (including the diode) within the converter can be reversed to provide a positive output voltage from a negative input voltage.
- **Application**
  - This configuration is used in specific cases where a negative voltage is required from a positive input, but it is not the most commonly used configuration.

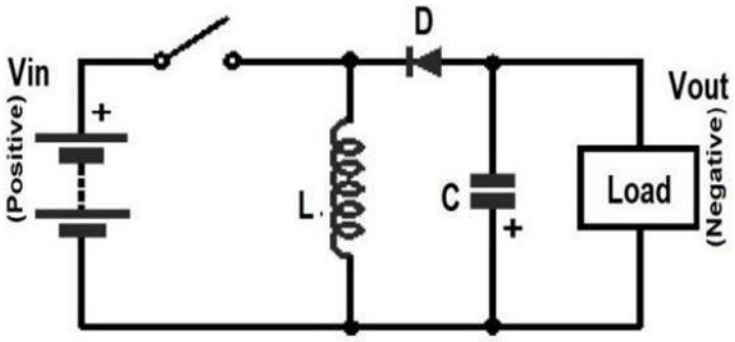


Fig I.13. DC/DC Buck-Converter (negative type).

b. +Vin, +Vout (Positive Output) Configuration:

- **Description**
  - In this configuration, both the input and output voltages have the same polarity (positive), but it requires additional components compared to the first configuration.
  -

- **Operation**
  - This configuration allows both input and output voltages to be positive, but to achieve this, the converter must incorporate more components.
  - The circuit design for this type of buck-boost converter may include additional switches, diodes, or other components to regulate the voltage and ensure proper conversion.
- **Application**
  - This type of converter is more commonly used when the application requires positive input and output voltages, and it can provide more flexibility in converting voltages.

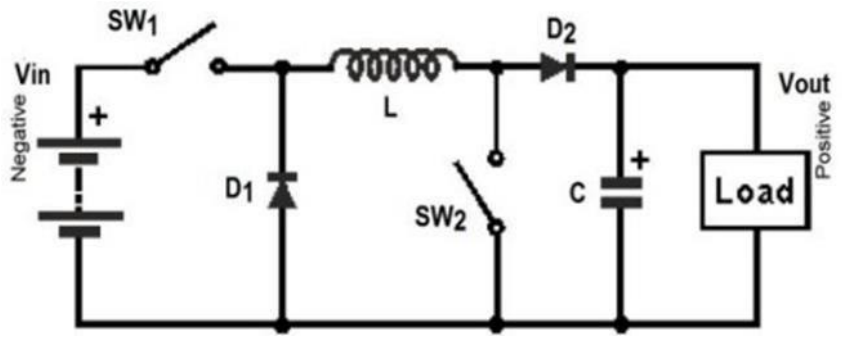


Fig I.14. DC/DC Buck-Converter (Positive type).

In this circuit, both switches operate simultaneously, meaning they are either both closed or both open. When the switches are open, the current builds through the inductor. At the appropriate point, the switches are closed. The inductor then supplies current to the load through a path that includes both diodes, D1 and D2. a DC-DC buck-boost converter is shown. The switching period is TT, and the duty cycle is D. Assuming continuous conduction mode of operation, when the switch is ON, the state-space equations are given by [1]:

$$\frac{dIL}{dt} = \frac{1}{L}(Vin) \quad (20)$$

$$\frac{dV0}{dt} = \frac{1}{C}\left(-\frac{V0}{R}\right) \quad (21)$$

0< t <dT, Q: ON

and when the switch is **OFF**

$$\frac{dIL}{dt} = \frac{1}{L}(V0) \quad (22)$$

$$\frac{dV0}{dt} = \frac{1}{C}(-iL - \frac{V0}{R}) \quad (23)$$

I.8. CONCLUSION

In this chapter, we explored the role of DC-DC converters, particularly Boost and Buck- Boost converters, in enhancing energy conversion efficiency in various electrical systems. The Boost converter was explained as a device that increases the input voltage to a higher output voltage, playing a crucial role in renewable energy systems like solar power. It relies on key components such as inductors, switches, diodes, and capacitors to store and release energy. On the other hand, the Buck-Boost converter was highlighted for its ability to both step up and step-down voltage, offering versatility for systems with varying voltage needs. Additionally, the impact of temperature and solar irradiance on solar cell performance was analysed, revealing that higher temperatures reduce the power generation capacity of cells, while solar irradiance determines the current and voltage output. The chapter concluded with a discussion on the ongoing challenges of improving conversion efficiency, emphasizing the need for further research in optimization and loss reduction for better performance in renewable energy systems.

Chaptre Ⅱ :

Synthesis of Direct⁄ (Indirect) MPPT Control Using P&O Algorithm

II.1. Introduction

To overcome the efficiency issue of solar panels and achieve maximum performance, it is necessary to optimize the design of all components within the photovoltaic (PV) system. In addition, the DC/DC converters used as an interface between the PV generator and the load must be optimized to continuously extract the maximum power, ensuring that the PV generator operates at its Maximum Power Point (MPP) without energy loss, using an MPPT controller. Consequently, this allows the system to deliver maximum power despite variations in load and environmental conditions (such as irradiance and temperature). A significant number of MPPT control techniques have been developed since the 1970s, starting from simple methods based on voltage and current feedback, to more advanced controllers using algorithms to calculate the MPP of the PV generator. Among the most commonly used methods is the Perturb and Observe (P&O) technique

II.2. direct connection between a PV generator and the charge

The principle of direct coupling between a PV generator (GPV) and the load is based on the transfer of output power from the photovoltaic source to the powered equipment without any intermediate system. This mode of operation is commonly referred to as "operation under the sun". The operating point is particularly influenced by several factors:

- the load,
- the operating conditions: irradiance, temperature,
- the type of connections used for the photovoltaic modules (parallel, series, or mixed) [6].

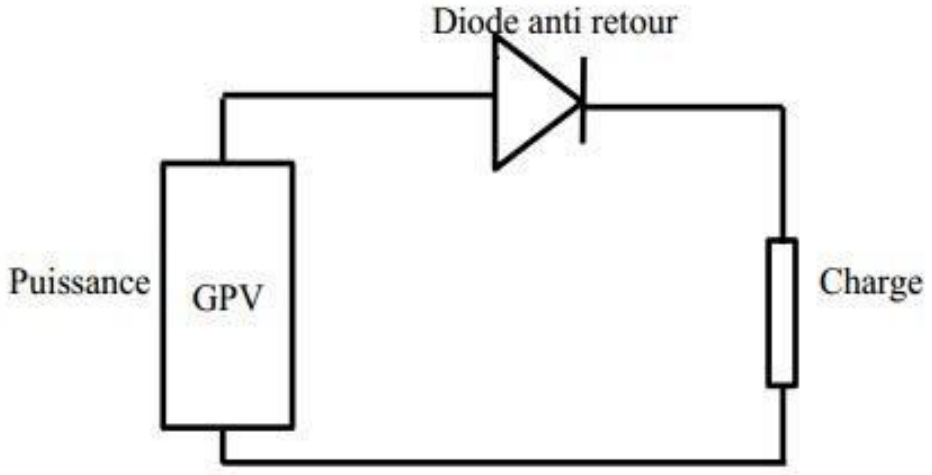


Fig II.1: Principle of Direct Coupling [22].

The main drawback of this type of connection is the direct dependency between the power supplied by the generator and the load. In fact, the power delivered by the photovoltaic module results from the intersection of the current-voltage (I–V) characteristic of the PV generator (GPV) and that of the load. The electrical characteristics of a GPV can change rapidly depending on solar irradiance, temperature, and, in the long term, cell aging. The aim of this study is to analyze the behavior of this setup for various types of loads and to present the results obtained from a direct connection. When a resistive load is directly connected to the PV generator, the operating point is determined by the intersection of the electrical characteristic of the load with that of the GPV.To ensure that the cells operate at their maximum power, the load must impose this optimal operating point. In the case of a resistive load, the load impedance ensure efficient use of the photovoltaic cells. However, this is not always the case. We assume that the nature of the load is direct current (DC). In fact, an alternating current (AC) load is not at all compatible with direct connection, as the GPV provides direct current. There are three types of DC loads: a purely resistive load, a voltage source-type load, and a current source-type load.

In Figure 2, we have shown the current-voltage (I–V) characteristics of a PV generator (GPV), as well as the I–V curves of the three types of DC loads [6].

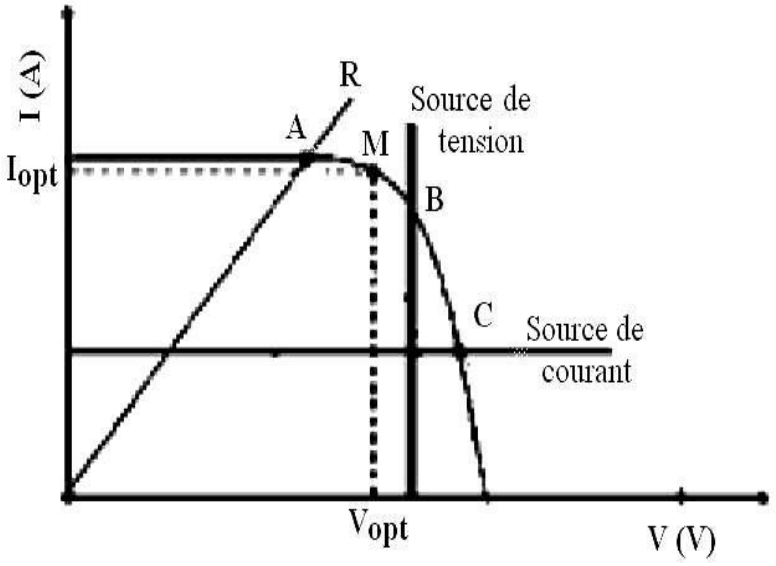


Fig II.2. Types of Loads in Direct Connection

We can identify point M as the operating point where the power delivered by the generator is maximum at an optimal current (Iopt) and an optimal voltage (Vopt). Next, we can find the

intersection point between the I-V characteristics of the generator and those of the three types of loads: -Point A for a resistive load, -Point B for a voltage source-type load, -Point C for a current source-type load, corresponding to power values lower than the maximum available power (Popt) [6].

To ensure that the generator operates as frequently as possible in its optimal regime, the commonly adopted solution is to introduce a static converter that will act as an adapter.

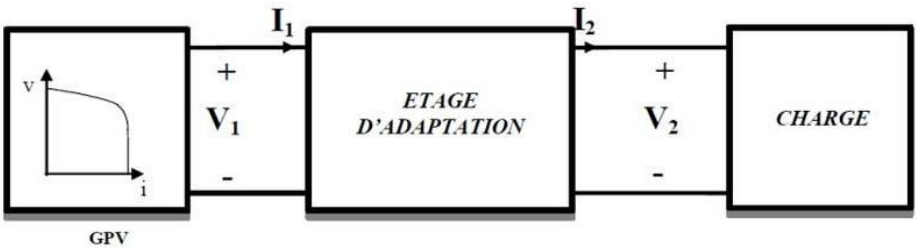


Fig II.3. PV Generator-Load Adaptation Stage [22].

II. 3. System Modeling

To ensure that the PV system operates at the maximum power points of its characteristics, there are specific control laws designed to meet this need. This control is referred to in the literature as Maximum Power Point Search or Maximum Power Point Tracking (MPPT) in English. The principle of these controls is to search for the Maximum Power Point (MPP) while maintaining a good adaptation between the generator and its load to ensure the transfer of maximum power [7]. The circuit under study consists of a photovoltaic generator (PVG), which will be optimized through a DC-DC converter controlled by an MPPT algorithm.

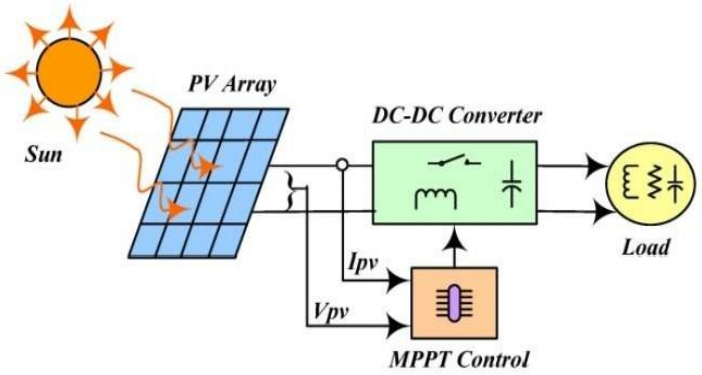


Fig II.4. Diagram of a photovoltaic system with MPPT control [24]

II. 4. Search for the Maximum Power Point

MPPT stands for Maximum Power Point Tracking. MPPT regulator scans voltage produced by the photovoltaic panel several times a day. Its purpose is to Find the maximum output point of the current supplied by the panel. Then to make sure always use this full power [8].

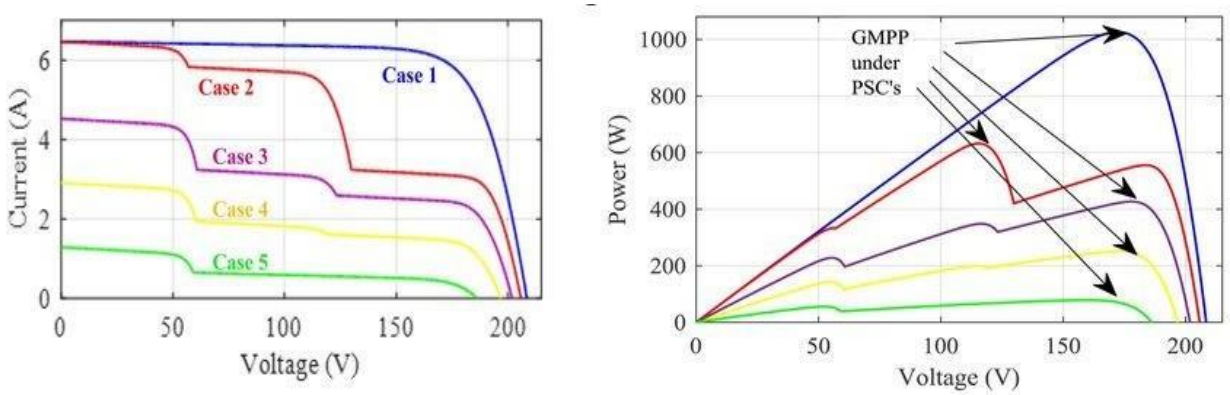


Fig II.5. The P-V, I-V characteristic [25].

II.5. Principle of MPPT control

In January 1968, A.F. Boehringer published the first MPPT control law adapted for a renewable energy source of the photovoltaic type. The control, based on an adaptive control algorithm, allows the system to operate at its maximum power point. Based on measurements of the current delivered by the photovoltaic panel (Ipv) and the voltage (Vpv), the method involves calculating the power at time ti and comparing it to the value stored at time ti-1. Subsequently, a new duty cycle is adjusted [13].

By definition, an MPPT control system combined with an intermediate adaptation stage enables a photovoltaic generator (PVG) to operate in such a way that it continuously produces its maximum power output. Thus, regardless of weather conditions (temperature and irradiance), the converter control places the system at its maximum operating point (Vmpp, Impp). The photovoltaic conversion chain is therefore optimized using a static converter controlled by an MPPT algorithm [9].

The MPPT control adjusts the duty cycle of the static converter using an appropriate electrical signal in order to extract the maximum power that the photovoltaic generator (PVG) can provide. The MPPT algorithm can be more or less complex depending on the method used to locate the Maximum Power Point (MPP).

In general, it is based on varying the duty cycle of the converter according to the evolution of its input parameters (current and voltage, and consequently the power of the PVG), until it reaches and locks onto the MPP [9].

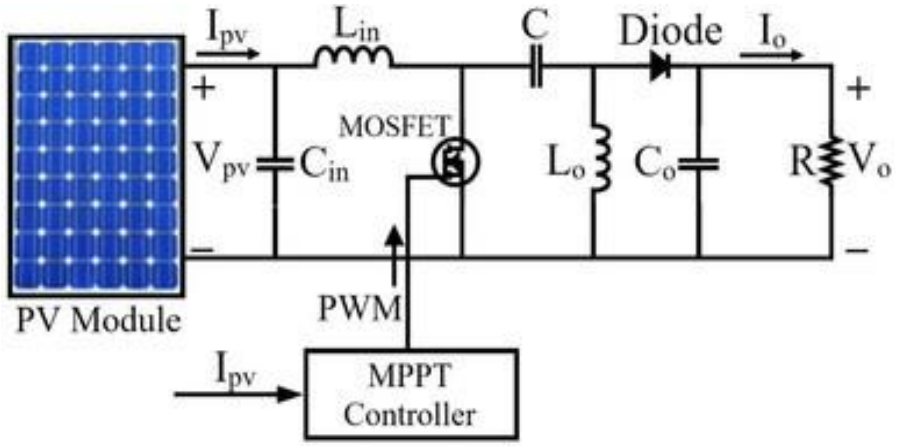


Fig II.6. Solar Energy conversion chain [23].

II.6. Evaluation Criteria for an MPPT Controller

The quality of an MPPT (Maximum Power Point Tracking) controller can be defined as the position of the system's operating point relative to the Maximum Power Point (MPP).The actual power delivered by the photovoltaic generator (PVG) depends on the control strategies applied at the converter level (MPPT, voltage control, direct connection, etc.).The efficiency of the resulting operating point, noted as η_{MPP} , serves to measure the effectiveness of the power converter's control strategy.η_{MPP} indicates the percentage of power loss of the PV module compared to the maximum power it could produce [20].

$$\eta_{MPPT} = \frac{P_{eff}}{P_{max}} \quad (24)$$

Where:

η_{MPPT}: Efficiency of the operating point

P_{eff}: The actual power delivered by the PV generator

P_{max}: The maximum potential power available from a PV panel

The performance evaluation of an MPPT controller is not limited to the η_{MPPT} parameter alone. Other equally important criteria are also used to assess the quality of the control strategy:

- **Simplicity and Cost:**

The MPPT controller should be simple in design, not energy-intensive, and have a reasonable operating cost, so that its use justifies any additional investment made [20].

- **Dynamic Response:**

The MPPT controller must have good dynamic performance to control the adaptation stage and ensure that, after changes in illumination or temperature, a new Maximum Power Point (MPP) is found as quickly as possible [20].

- **Flexibility:**

Regardless of the operating conditions, the MPPT controller must be precise and stable. It should be designed to operate accurately and robustly across different types of panels, without requiring significant modifications [20].

- **Competitiveness Across a Wide Power Rang:**

The MPPT controller used must track the MPP generated by the photovoltaic module, regardless of the level of sunlight. The controller is considered competitive if the MPP is reached with a low static error, which corresponds to the operating point's position relative to the MPP, over a wide power range [20].

II.7. MPPT Classification

We can generally classify MPPT control methods according to the type of electronic implementation: analog, digital, or hybrid. However, it is more relevant to classify them based on the type of search they perform and the input parameters used by the MPPT controller. Although a large number of scientific publications present MPPT control strategies with varying levels of complexity, we will focus on a few that best represent each type of algorithm [10].

7.1. Classification of MPPT Controls Based on Converter Parameters

7.1.1 MPPT Control Based on the Input Parameters of the Converter

This type of MPPT control searches for the Maximum Power Point (MPP) based on the evolution of the power supplied by the PV generator (PVG). The control therefore requires measuring the current and voltage at the input of the converter. Other types of MPPT control are based on regulating the current of the PVG, assuming that the current is proportional to the power. This approach makes it possible to get as close as possible to the optimal current (Iopt). Since this type of control requires only one sensor, it is easier to implement and low cost [11].

7.1.2 MPPT Control Based on the Output Parameters of the Converter

There are also algorithms based on the output parameters of DC-DC converters. For example, MPPT controls based on the maximization of output current are mainly used when the load is a battery. In all systems that use output parameters, an approximation of Pmax is made through the efficiency of the converter. In summary, the better the conversion stage, the more accurate this approximation becomes. However, in general, all systems using only one sensor are inherently not very precise. Most of these systems were originally designed for space applications [12].

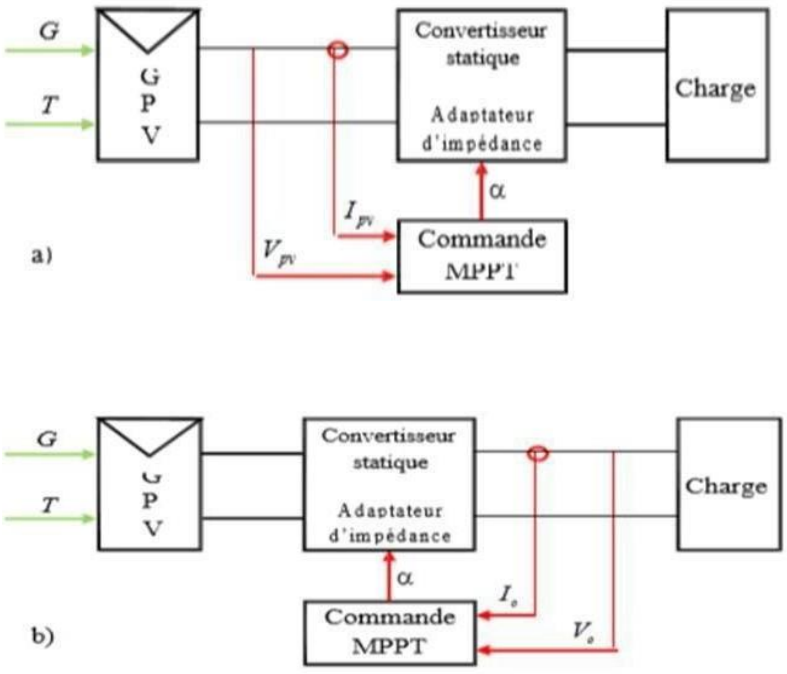


Fig II.7. Principle of Impedance Matching via MPPT

a) Using Input Parameters

b) Using Output Parameters

7.2. Classification of MPPT Control Based on the Type of Search

7.2.1. Indirect Methods

This type of MPPT control determines the optimal operating point (MPP) from the currents, voltages, or powers measured in the system. It can therefore react to unpredictable changes in the operation of the PV generator (PVG). Generally, these procedures are based on a search algorithm, through which the maximum of the power curve is determined without interrupting operation. To do this, the operating point voltage is incremented at regular intervals. If the output power increases, the search direction is maintained for the next step; otherwise, it is reversed [9].

The actual operating point then oscillates around the MPP. This basic principle can be preserved by other algorithms to prevent misinterpretations. These errors can arise, for example, from a wrong search direction, due to a power increase resulting from a sudden rise in irradiation. The determination of the PV generator's power value, essential for tracking the MPP, requires measuring the generator's voltage and current and multiplying these two variables. Other algorithms rely on introducing small-signal sinusoidal variations into the switching frequency of the converter to compare the AC and DC components of the PV voltage, and thus place the operating point of the PV generator as close as possible to the MPP.

The advantage of this type of control is its accuracy and fast response.

7.2.2. direct Methods

The instantaneous values of the PV output voltage or current are generally used to generate the control signals, and the algorithm is based on the variation of these measurements. The advantage of these algorithms is that they do not require prior knowledge of the characteristics of the PV panels. Therefore, they can respond to unpredictable changes in the PV's operation. For this reason, the operating point voltage is incremented at regular intervals. If the output power increases, the search direction is maintained for the next step; otherwise, it is reversed [13].

II.8. Maximum power point search technique

Several techniques are mentioned to track the maximum power point:

- Perturb and Observe (P&O).
- Incremental conductance (CI).
- Fuzzy Logic Controller (FLC).
- Genetic algorithm (GA).

II.9. Perturb & Observe (P&O)

Typically, P&O method is used for tracking the MPP. In this technique, a minor perturbation is introduced to, cause the power variation of the PV module. The PV output power is periodically measured and compared with the previous power. If the output power increases, the same process is continued otherwise perturbation is reversed. In this algorithm perturbation is provided to the PV module or the array voltage.

The PV module voltage is increased or decreased to check whether the power is increased or decreased. When an increase in voltage leads to an increase in power, this means the operating point of the PV module is on the left of the MPP.Conversely, if an increase in voltage leads to a decrease in power, this means the operating point of the PV module is on the right of the MPP.

When the MPPT charge controller is connected between the PV module and battery, it measures the PV and battery voltages. After measuring the battery voltage, it determines whether the battery is fully charged or not. If the battery is fully charged (12.6 V at the battery terminal) it stops charging to prevent battery over charging. If the battery is not fully charged, it starts charging by activating the DC/DC converter.

The microcontroller will then calculate the existing power P_{New} at the output by measuring the voltage and current, and compare this calculated power to the previous measured power P_{Old}. If Pnew is greater than P_{Old}, the MPPT duty cycle is increased to extract maximum power from the PV panel. If P_{New} is less than P_{Old}, the duty cycle is reduced to ensure the system to move back to the previous maximum power. This MPPT algorithm is simple, easy to implement, and low cost with high accuracy.[16]

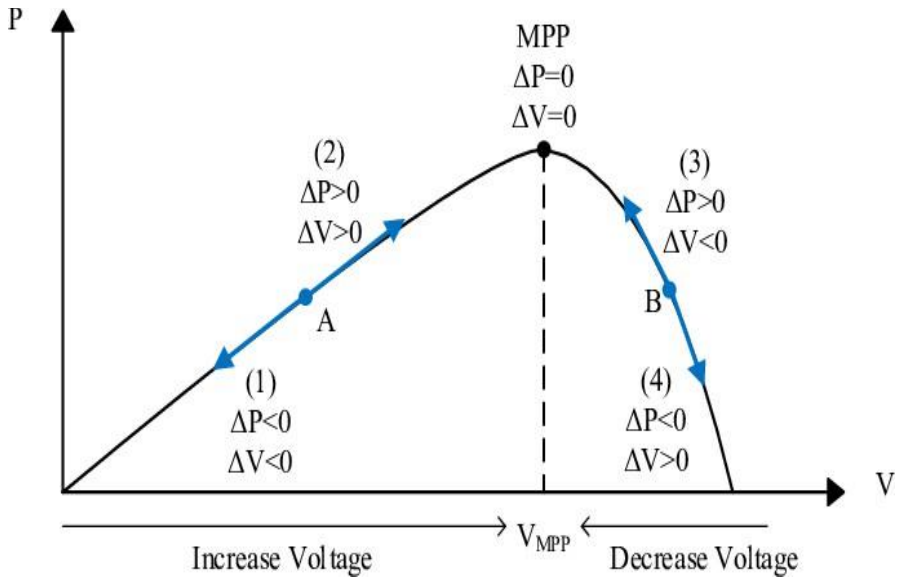


Fig II.8. Tracking the (MPP) using the Perturb and Observe (P&O) method [26].

Figure II.8. shows the block diagram of the implementation of the P&O algorithm. First, the current voltage and current of the PV system are measured. After that, the product of the voltage and current gives the actual power of the PV module. Then, the state is checked to determine whether $\Delta P = 0$ or not. If this condition is met, then the operating point is at the MPP (Maximum Power Point) [21].

If this condition is not met, another condition is checked, namely whether $\Delta P > 0$. If this condition is met, it will then be checked whether $\Delta V > 0$. If that is also satisfied, it indicates that the operating point is to the left of the MPP. If the $\Delta V > 0$ condition is not satisfied, it indicates that the operating point is on the right side of the MPP [21].

This process is continuously repeated until the MPP is reached. Thus, at all times, there is a trade-off between the step size and the sampling rate in the P&O algorithm [21].

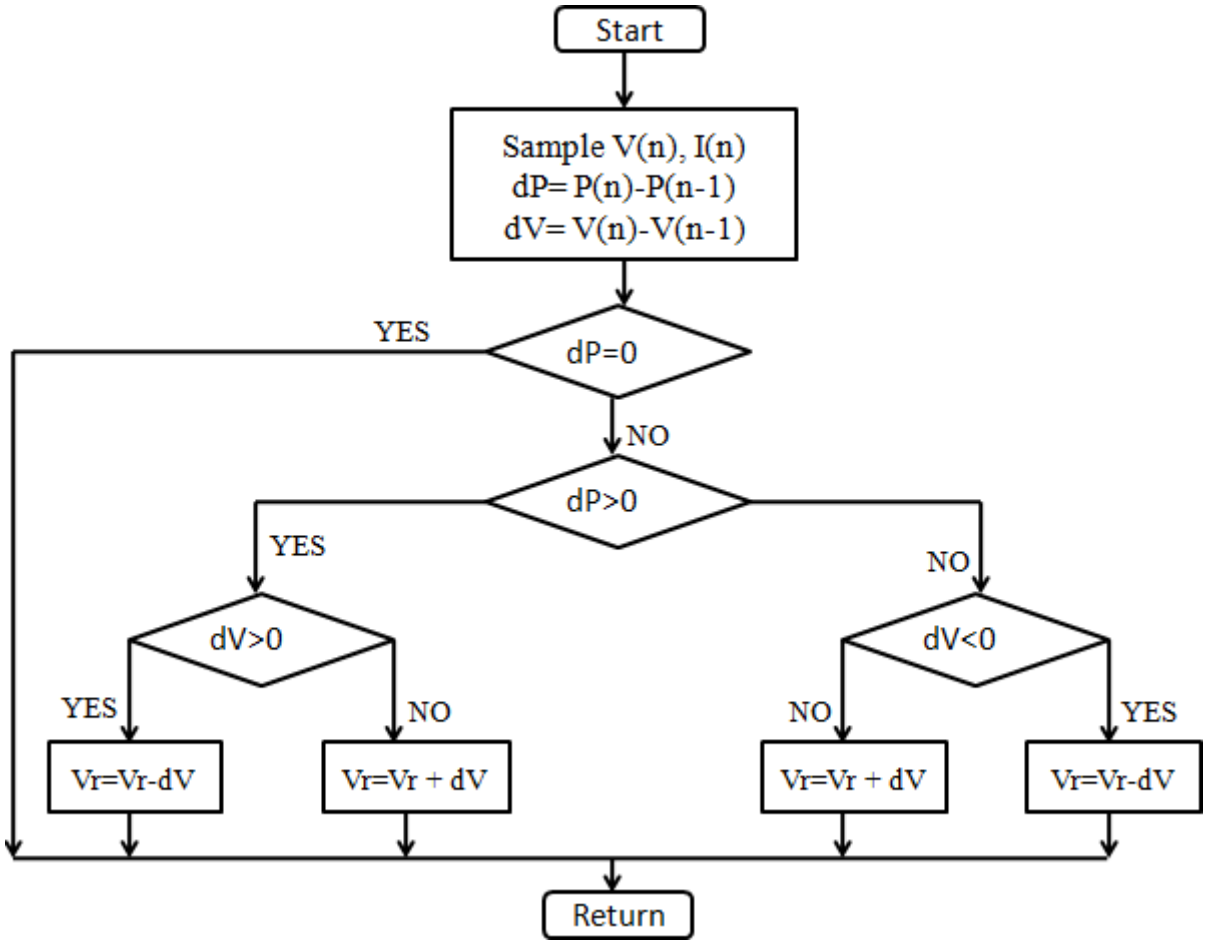


Fig II.9. Flowchart of P&O method [27].

The P&O method is now widely used because of its ease of implementation; however, it presents some issues related to the oscillations around the MPP that it causes in steady state, since the search procedure for the MPP must be repeated periodically, forcing the system to oscillate continuously around the MPP once it has been reached. These oscillations can be minimized by reducing the value of the perturbation step. However, a small step value slows down the search for the MPP, so a compromise must be found between accuracy and speed which makes this control difficult to optimize [7].

The algorithm is developed in such a manner that it sets a reference voltage of the module corresponding to the peak voltage of the module. A PI controller is used to move the operating point

of the module to that particular voltage level. It is observed that there is some power loss due to this perturbation and it also fails to track the power under fast varying atmospheric conditions. But still this algorithm is very popular because of its simplicity [15].

Advantages

- Simple to implement with low computational requirements.
- Works effectively under steady atmospheric conditions.

Disadvantages

- Oscillates around the maximum power point (MPP), leading to potential losses.
- Struggles under rapidly changing conditions, causing delays in tracking the optimal point.[17]

Performance Comparaison

- **Efficiency:** Studies show that the INC algorithm is generally more efficient than P&O, as it better maintains operation near the MPP throughout varying environmental conditions. This efficiency translates to increased power output from PV systems in real-world installations, especially during fluctuating weather
- **Tracking Speed:** INC often demonstrates faster response times when atmospheric conditions change. It can quickly ascertain whether the power output has peaked and halt unnecessary adjustments, minimizing energy losses compared to P&O, which may continue to oscillate around the MPP
- **Implementation Considerations:** While P&O is favored for its simplicity and lower costs, INC is preferred in applications where performance is critical and environmental conditions are highly variable. Simulation studies in MATLAB/Simulink have shown that INC outperforms P&O under defined conditions, affirming its effectiveness [17].

Mppt Algorithm	**P&O**
Complexity	Base
Identification of PV panel parameters	Not necessary
Number of iterations	45
Convergence speed	Average
Accuracy	95%

Table II.1: Comparison of P&O and INC MPPT Techniques

II.10. Conclusion

In this chapter, we have started the most important and delicate part of this thesis. It involves presenting the principle of maximum power point tracking (MPPT) while providing the different classifications of MPPT controllers. we implemented an MPPT control application on a PV system consisting of a PV generator, a DC-DC converter, and a load. We then presented the results for varying temperature and irradiance conditions. The simulation results demonstrate satisfactory performance in terms of voltage, generated power, and load behavior. We have detailed the P&O method, which we will develop in the next chapter. The advantages and disadvantages of the method have been discussed. The simulation of a photovoltaic system under various conditions, with the application of the studied MPPT control methods, is addressed in the following chapter.

Chaptre III:

Application of PR Control for PV Module Voltage Regulation

III.1. Introduction

The integration of photovoltaic (PV) systems into modern energy infrastructures has grown significantly in recent years, driven by the global push for cleaner, more sustainable energy sources. As these systems become more widespread, the need for efficient and reliable control strategies becomes increasingly critical—particularly in the regulation of voltage at the module or string level. Maintaining a stable and precise output voltage is essential for maximizing energy conversion efficiency, ensuring safe operation, and enabling effective interaction with downstream power electronics and grid interfaces. Traditional control methods, such as PI (Proportional-Integral) controllers, have been widely used in PV systems due to their simplicity and ease of implementation. However, their limitations become apparent when dealing with alternating components in the system dynamics or when precise regulation is required under time-varying irradiance and temperature conditions. This is where Proportional Resonant (PR) controllers offer a compelling alternative. PR controllers are particularly effective in regulating sinusoidal signals and rejecting periodic disturbances. While they are commonly employed in current control for grid-tied inverters, their capabilities can also be extended to voltage regulation in PV modules, especially where the control objective involves tracking or rejecting low-frequency oscillations. By introducing high gain at a specific frequency without affecting the system's performance at other frequencies, PR controllers enable more robust and precise control, even in challenging environmental conditions. This chapter explores the application of Proportional Resonant control techniques in the context of photovoltaic module voltage regulation. It begins with a brief overview of PV module behavior and control challenges, followed by the theoretical background of PR control. The chapter then presents the design methodology, simulation results, and practical considerations for implementing PR controllers in PV systems. Through this exploration, we aim to demonstrate the advantages of PR control in enhancing the stability and performance of PV voltage regulation

III.2. PROPORTIONAL RESONANT CONTROLLER

In this section, the structure of the PR controller is presented, justified by the classical PI control.

A. PI Controller

A PI controller generates two control actions then combines them to form the signal to be applied to the plant

$$U(s) = U_i(s) + U_p(s) \quad (25)$$

In (25), $U_i(s)$ is the integral control action and $U_p(s)$ is the proportional action. These are defined as

$$U_i(s) = \frac{K_i}{s} E(s) \qquad U_p(s) = K_p E(s)$$

Hence, the transfer function of a PI controller is given by

$$_{pi}(s) = \frac{U(s)}{E(s)} = \frac{K_i}{s} + K_p \tag{26}$$

$$= K_i C(s) + K_p C_p(s) \tag{27}$$

with seemingly obvious definitions for Ci (s) and Cp(s). The fundamental role of a PI controller is to guarantee zero steady-state error when the reference and the disturbances acting on the plant are piecewise constant. This is achieved by the integral action alone, and the proportional action is zero in steady state. Hence, the most fundamental control action is the integral action and it could, at least in principle, be applied by itself to achieve this goal for a large class of processes.

Indeed, any stable minimum phase process can be controlled by a purely integral controller, provided that sufficiently small integral gain is used. However, transient performance and stability margins with purely integral control could, and usually would, be unacceptably poor. Hence, an additional term is added to the control law to improve transient performance and stability margins with purely integral control could, and usually would, be unacceptably poor. Hence, an additional term is added to the control law to improve transient performance and robustness, and to achieve closed-loop stability for a larger class of processes. This additional control action is the proportional action, which can be seen as the derivative of the most fundamental integral action, that is

$$C(s) = sC_i(s) \tag{28}$$

B. PR controller

For inverters, the controller deals with sinusoidal signals, which makes it difficult to design the controller with the correct gain that is able to regulate the performance at the fundamental frequency and also to reject harmonic disturbances. PI controllers, having a pole (with an infinite gain) at the zero frequency, are not able to eliminate the steady-state error at the fundamental frequency. While PI controllers have infinite gain at 0 Hz, PR controllers have infinite gain at their resonant frequency ω_0 [28].

The transfer function of this controller with sinusoidal internal model is The PR current controller GPR(s) is represented by:

$$C_r(s) = \frac{s}{s^2+\omega_r{}^2} \quad (29)$$

where ω_r is the frequency that must be followed and/or rejected. The integral control action Ci (s) is a particular case of the resonant control action (29), obtained by setting ωr = 0. In vibration control, the fundamental control action is slightly more general [29].

According to IMP (international model), if the closed-loop stability is guaranteed, then the resonant controller defined in (29) ensures zero steady state error for sinusoidal tracking (disturbance rejection) at frequency ω_r.This PR controller described by is considered an ideal controller and as shown from Bode diagram that it has a theoretically infinite gain at the frequency $\omega_r$which enables it to ensure zero steady-state error at this frequency only and introduces no gain or phase shift at other frequencies. This infinite gain of the ideal controller may lead to difficulty in the implementation with either analogue or digital system.

III.3. Characteristics of the PR controllers

Proportional Resonant (PR) Controllers are widely used in control systems, particularly in applications involving **sinusoidal reference tracking** or **disturbance rejection at specific frequencies**. Their main objectives are:

3.1. Perfect Tracking of Sinusoidal Signals (Zero Steady-State Error)

- The key objective of PR controllers is to **eliminate steady-state error** when tracking or rejecting **sinusoidal signals**, especially at a specific frequency (often the fundamental frequency in power systems, like 50/60 Hz).
- Unlike PI controllers, which are effective only for DC signals, PR controllers are designed to **have infinite gain at a given frequency** (resonant frequency), ensuring **perfect tracking or rejection** at that frequency.

3.2. Disturbance Rejection at Specific Frequencies

- PR controllers are effective in rejecting **sinusoidal disturbances** (harmonics, grid disturbances, etc.) that occur at known frequencies.

- This makes them especially useful in **grid-connected converters**, **active filters**, and **inverters**.

3.3. High Selectivity with Minimal Impact on Other Frequencies

- PR controllers provide **high gain only at the resonant frequency**, leaving the system behavior largely unaffected at other frequencies.
- This selective behavior allows precise control without destabilizing the system.

3.4. Suitability for AC Systems and Power Electronics

- In applications like **AC current control**, **inverter control**, and **grid synchronization**, PR controllers are preferable over PI controllers because they are designed for **AC signal regulation**.

3.5. Simple Implementation in Stationary Reference Frame

- PR controllers can be implemented in the **αβ stationary frame**, avoiding the need for transformation to and from the rotating dq frame, which is common in PI-based control.

Objective	**Description**
Zero steady-state error for AC signals	Infinite gain at a specific frequency (resonance)
Sinusoidal disturbance rejection	Effective against harmonics or grid-related disturbances
Frequency-selective control	High gain at resonant frequency only
Stationary-frame implementation	Useful in αβ-frame without coordinate transformation
Common in power electronics	Widely used in inverters, UPS, grid-connected converters, etc.

Table III.1: PR Controller Objectives

III.4. Proposed Controller

A PI controller is a type of feedback controller that combines proportional and integral control actions. Its transfer function in the Laplace domain is:

$$K_p + \frac{K_i}{s} \tag{30}$$

A PI controller implemented in the positive-sequence synchronous frame is not equivalent to a PR controller in the stationary frame

$$K_p + \frac{K_i s}{s^2+\omega^2_0} \tag{31}$$

A PR controller comprises of two parts, i.e., the proportional and resonant parts, expressed by the equation below:

$$C_{PR}(s) = K_p + K_i\left(\frac{s}{s^2+\omega^2_0}\right) \tag{32}$$

Where, KP is the proportional gain term, KI is the integral gain term and ω_0 is the resonant frequency.

let us apply the same principle as in PI controllers, expressed in (27). Taking the derivative of the fundamental (resonant) control action yields

$$C_P(s) = K_r C_r(s) + K_p C_p(s) \tag{33}$$

$$C(s) = sC_r(s) \tag{34}$$

With:

$$C_r(s) = \frac{s}{s^2+\omega^2_0} \tag{35}$$

which added to the resonant control action results in the PR controller

$$C_{PR}(s) = K_r \frac{s}{s^2+\omega^2_0} + K_P \frac{s^2}{s^2+\omega^2_0} \tag{36}$$

where Kr, Kp ∈ R are parameters to be tuned

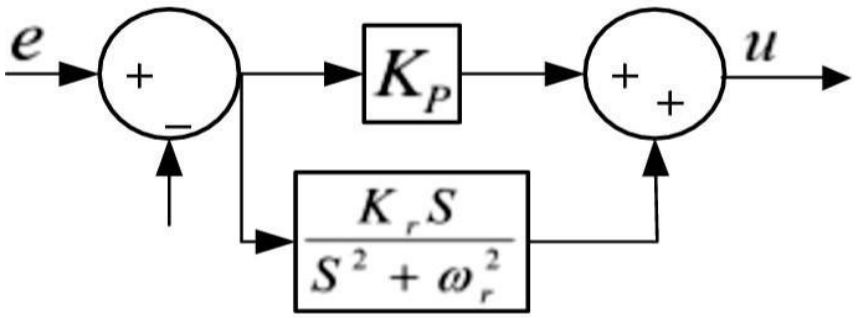
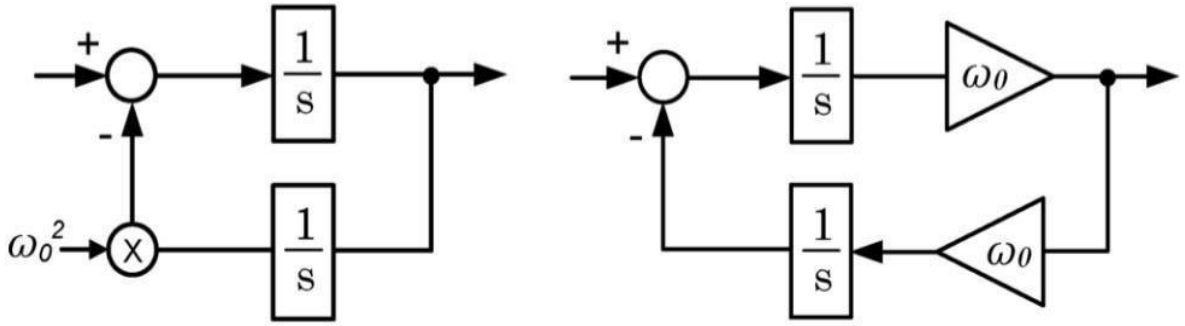


Fig III.1.PR controller [30]

With KP and kI being the controller's gain constants, the combination of a PI controller in the positive-sequence synchronous frame and another PI controller in the negative-sequence synchronous frame is, in fact, equivalent to a PR controller in the stationary frame [30].



SOGI scheme 1: $\frac{s}{s^2+\omega_0^2}$ SOGI scheme 2: $\frac{\omega_0 s}{s^2+\omega_0^2}$

Fig III.2. Resonant controller schemes [30]

PR controllers have narrow bandwidths around the resonant frequency. Some authors, such as those in Refs, compare the performance of using PI controllers versus PR controllers. Moreover, for large values of ω_0, the delay introduced by the sampling time and modulation can negatively affect system performance and stability. Adding a phase lead to the standard PR transfer function can help compensate for this delay.

The ideal resonant term on its own in the PR controller provides an infinite gain at the ac frequency ω_0 and no phase shift and gain at the other frequencies. The KP term determines the dynamics of the system; bandwidth, phase and gain margins. Unfortunately, the ideal PR controller acts like a network with an infinite quality factor, which is hard to implement the PR controller in reality. Firstly, the infinite gain introduced by PR controller leads to an infinite quality factor which cannot be achieved in either analog or digital system. Secondly, the gain of PR controller is much reduced at other frequencies and it is no adequate

corrector can track the sinusoidal reference and mitigate the harmonics better than PI controller, moreover, it allows us to have a unit power factor despite the addition of the reactive load and especially without influencing the pace of the reactive power and without introducing any instantaneous phase difference between the voltage and the current injected into grid.

III.5. Criterion for Evaluating MPPT Performance in PVG

a) efficiency criterion

When evaluating a photovoltaic (PV) energy system, the primary efficiency to consider is the one related to maximizing the power output of the PV generator. This efficiency, assessed at the PV generator's output, reflects how closely the system operates to the maximum power point (MPP). It serves as an indicator of the effectiveness of the control strategy in steering the operating point of the PV generator toward the MPP. This metric is commonly referred to as the **MPPT (Maximum Power Point Tracking) efficiency**, and it is defined by the following equation:

$$E_f = \frac{\sum_{i=1}^{M} p_{pv}(i)}{\sum_{i=1}^{M} p_{max}(i)} \times 100 \qquad (37)$$

b) Energy consumption criterion

Integral Absolute Control Signal (IACS) is a method for evaluating the energy consumption of a control signal over time

$$IAC(u) = \int_0^{\infty} |(t)| dt \quad (38)$$

U(t) is the control signal (output of the controller)

Interpretation

- **Lower IACS** → the controller is using less energy or exerting less effort to control the system.
- **Higher IACS** → possibly more responsive control, but at the cost of higher energy use or actuator activity.

III.6. Simulation Results

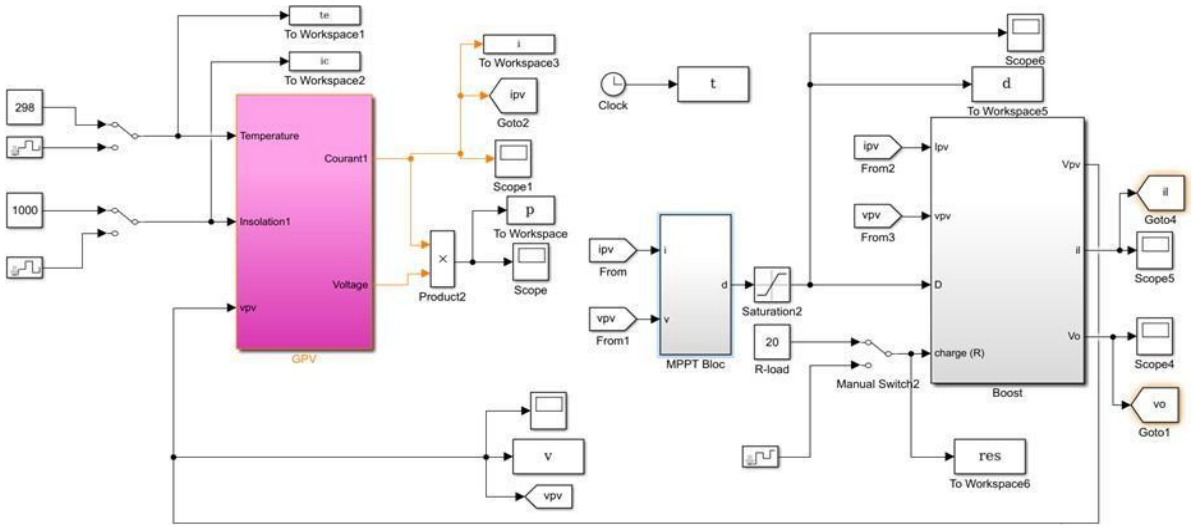


Fig III.3. Synoptic diagram of the control loops

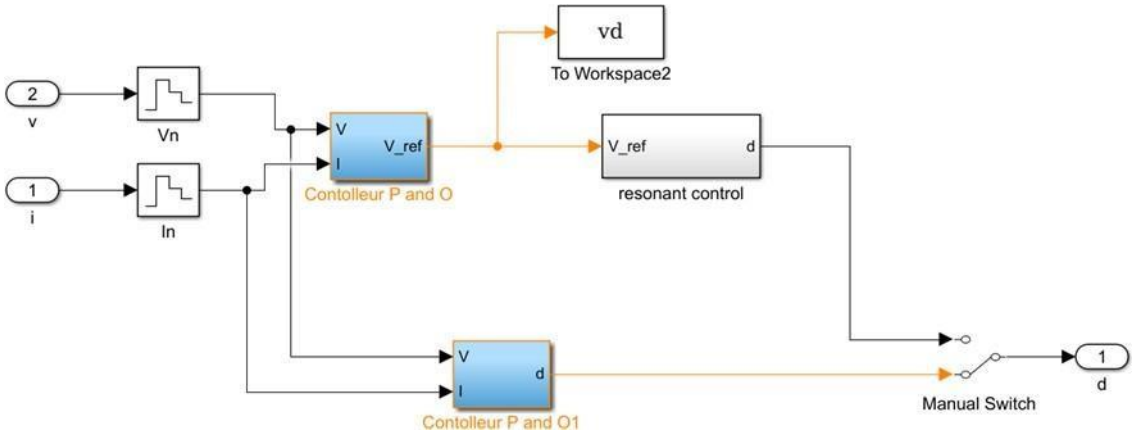


Fig III.4. Block diagram of the P&O and PR controllers.

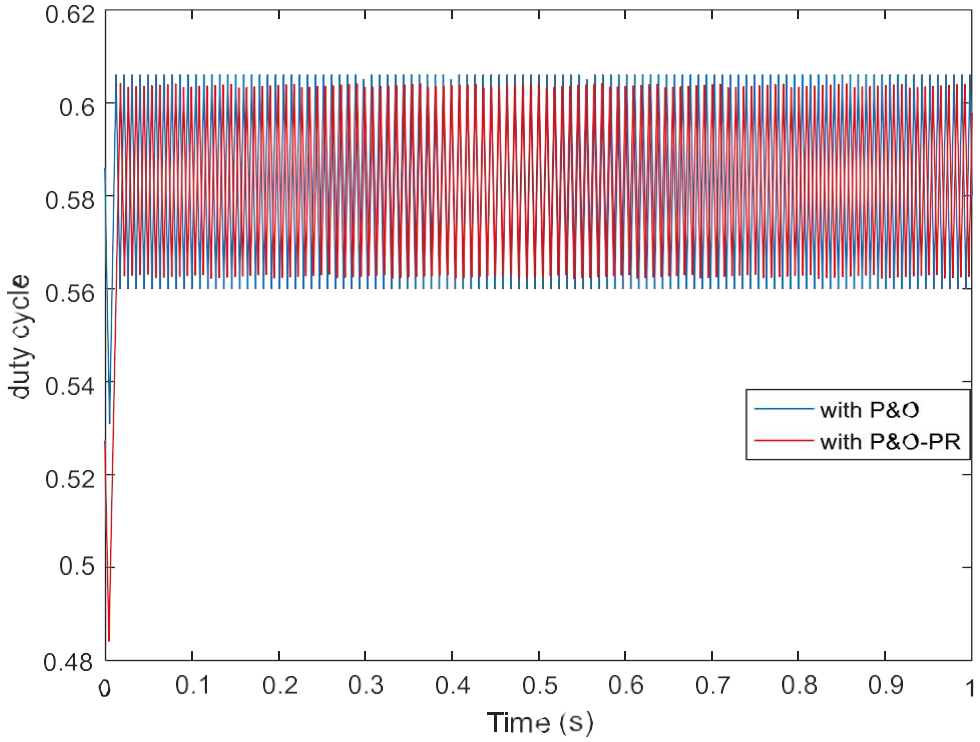


Fig III.5. The duty cycle of PV module with P&O and P&O_PR.

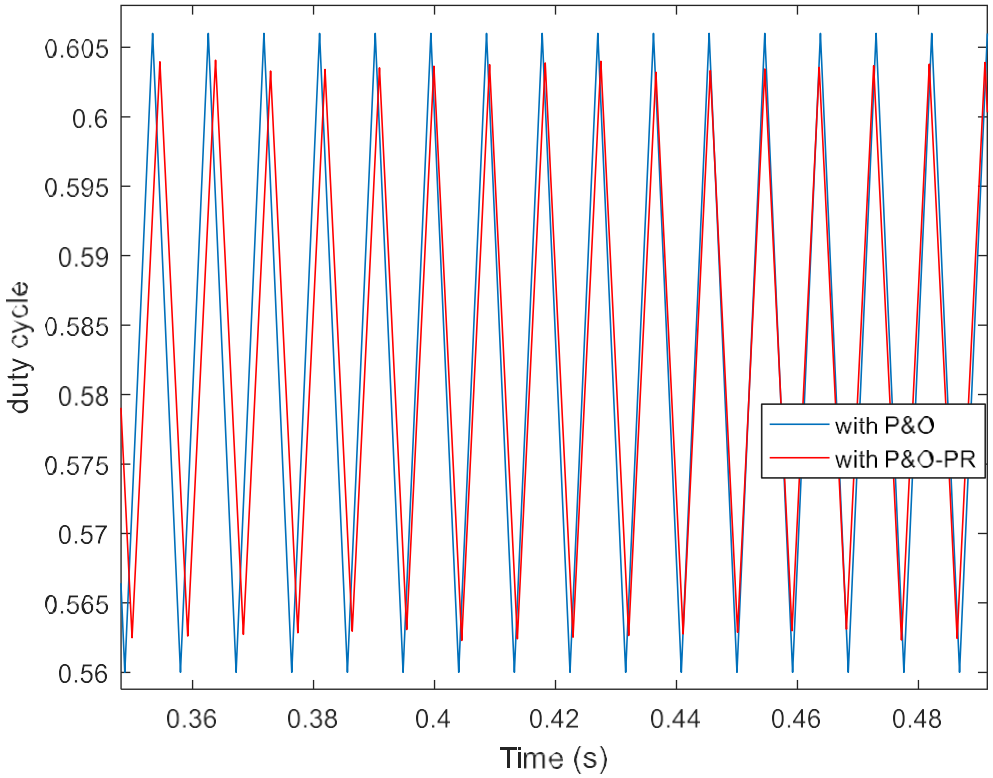


Fig III.6. Zoom of the duty cycle of PV module with P&O and P&O_PR.

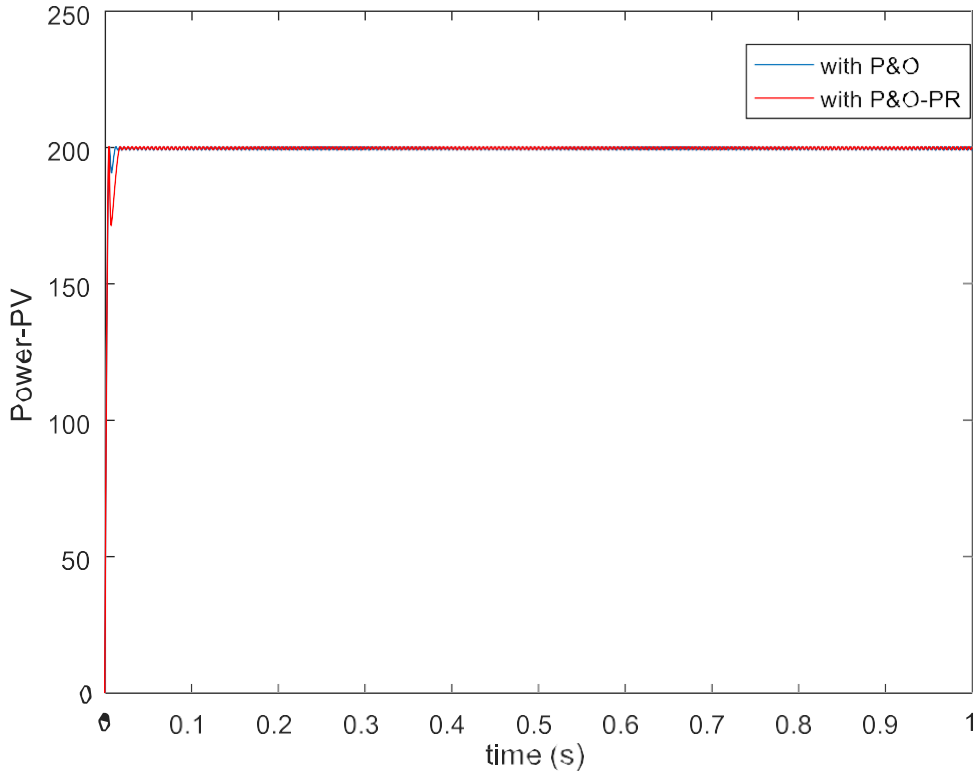


Fig III.7. The power of PV module with P&O and P&O_PR

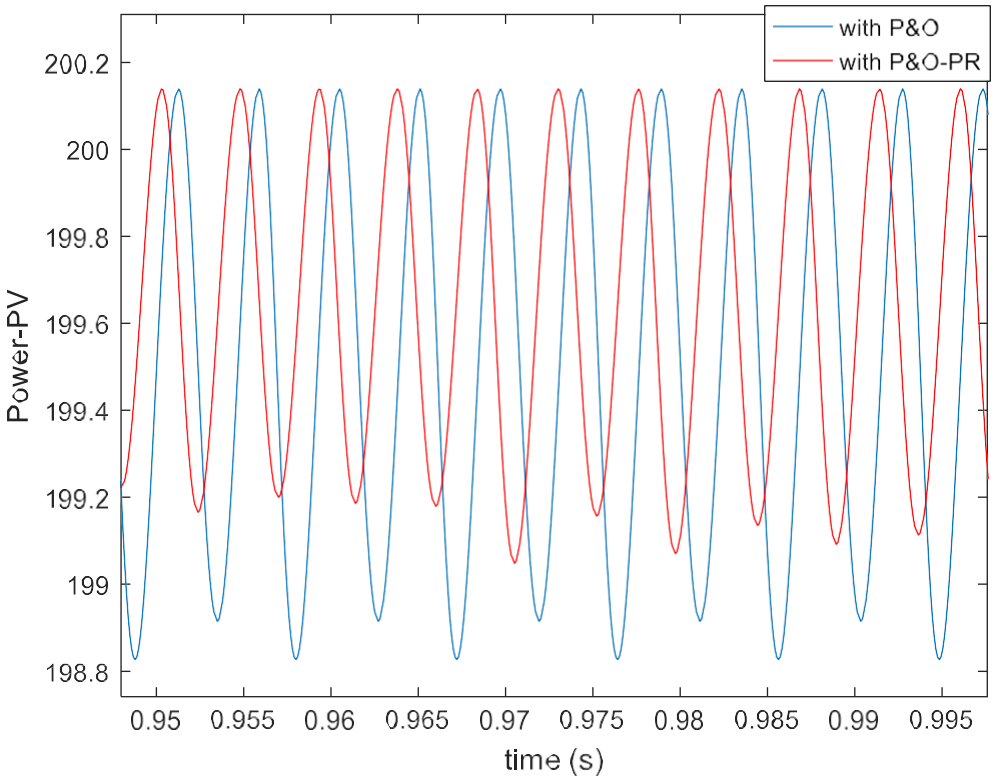


Fig III.8. Zoom at the power of PV module with P&O and P&O_PR

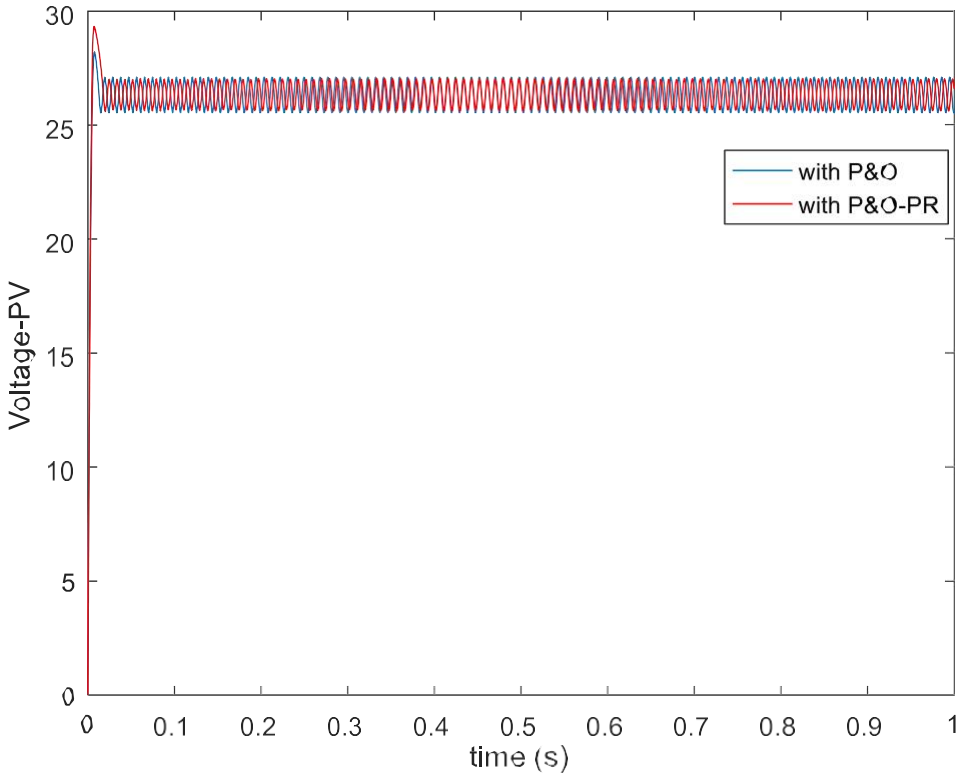


Fig III.9. The Voltage of PV module with P&O and P&O_PR

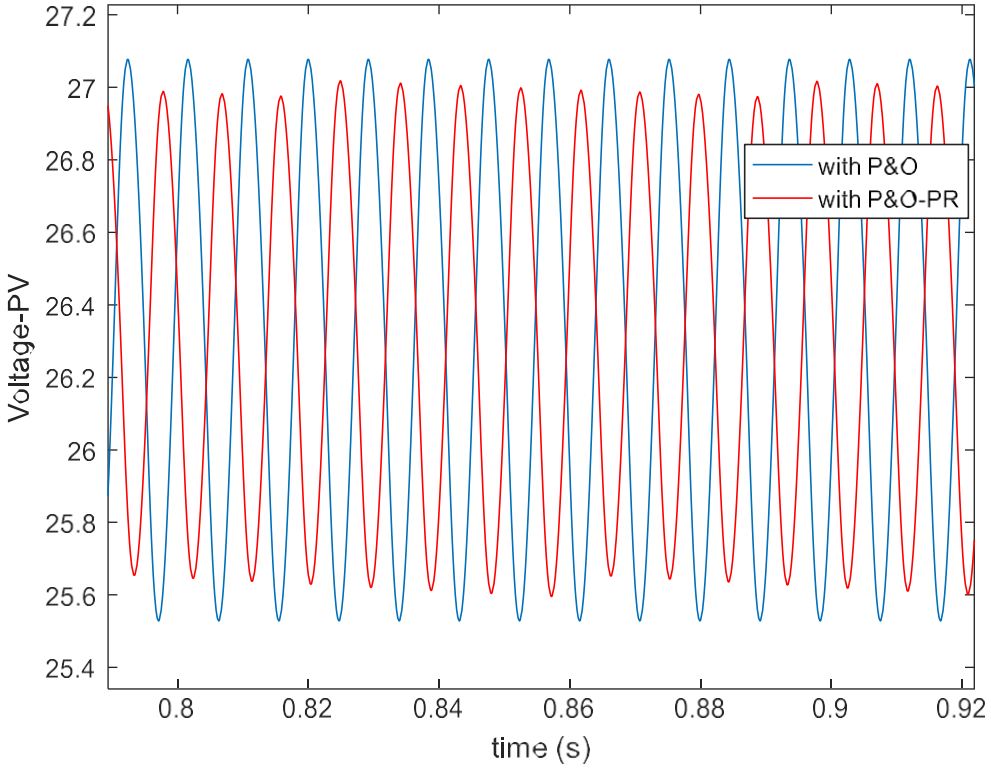


Fig III.10. Zoom at the Voltage of PV module with P&O and P&O_PR

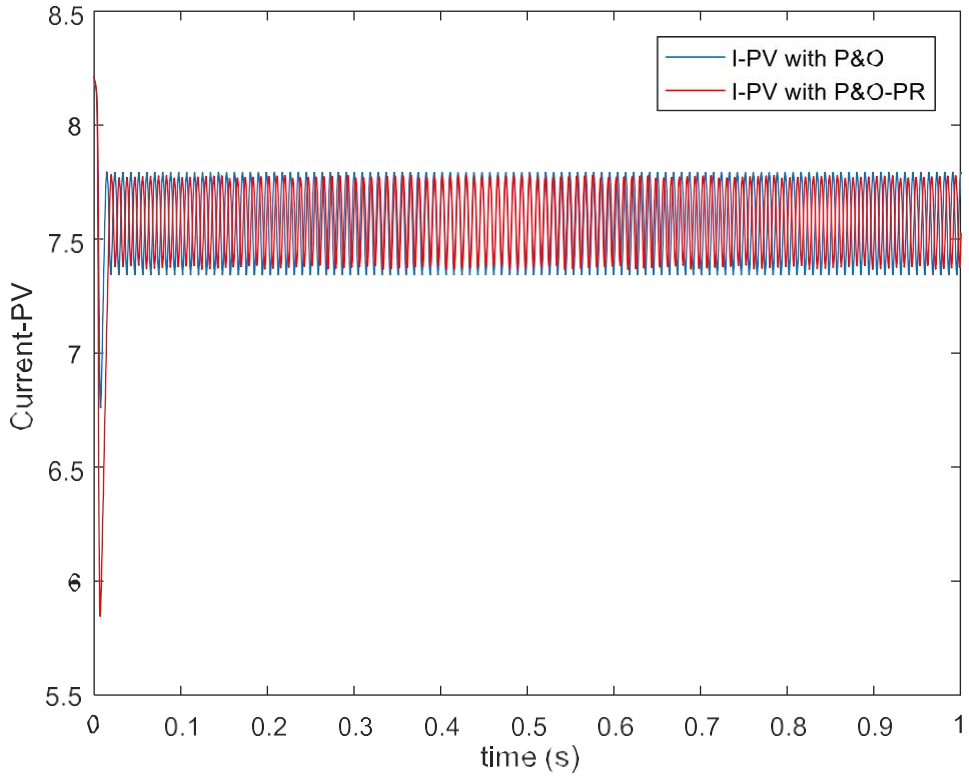


Fig III.11. The Current of PV module with P&O and P&O_PR

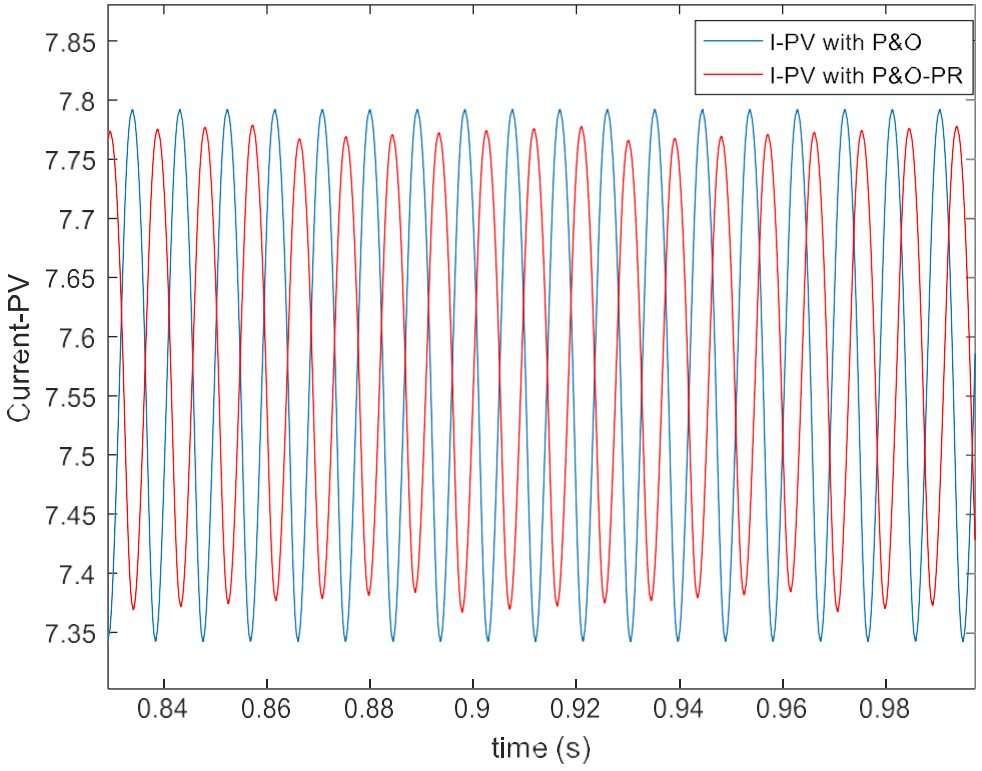


Fig III.12. Zoom at the Current of PV module with P&O and P&O_PR

Variable Temperature [288 303 318 298 308]

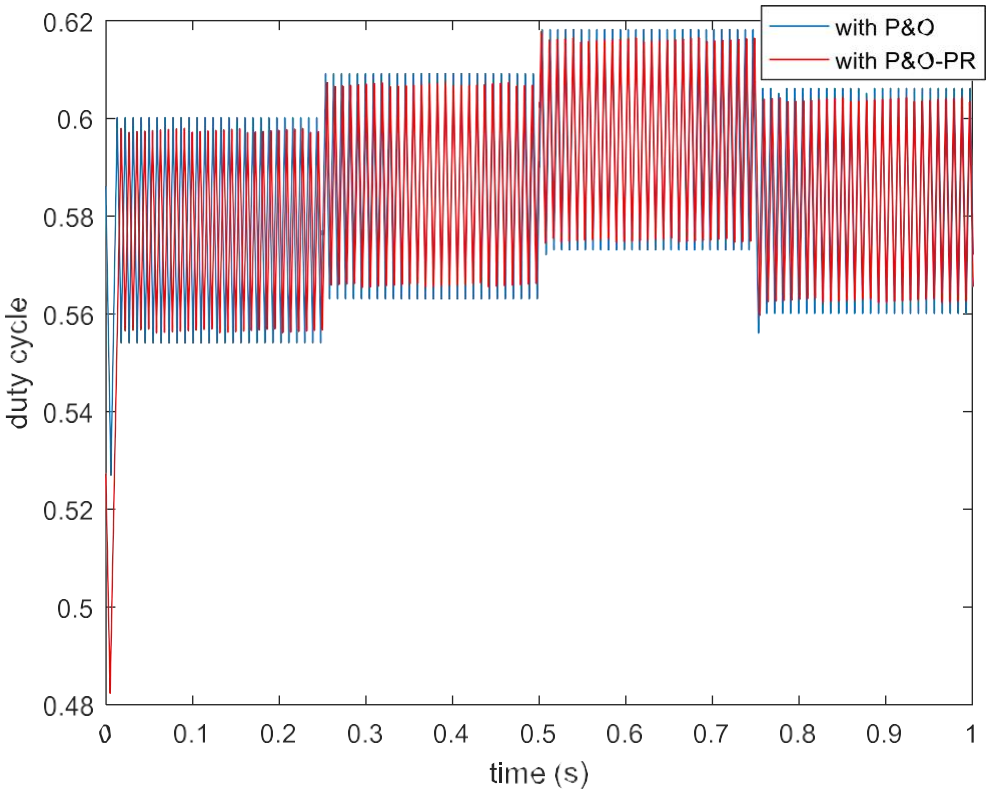


Fig III.13. The duty cycle of PV module with P&O and P&O_PR

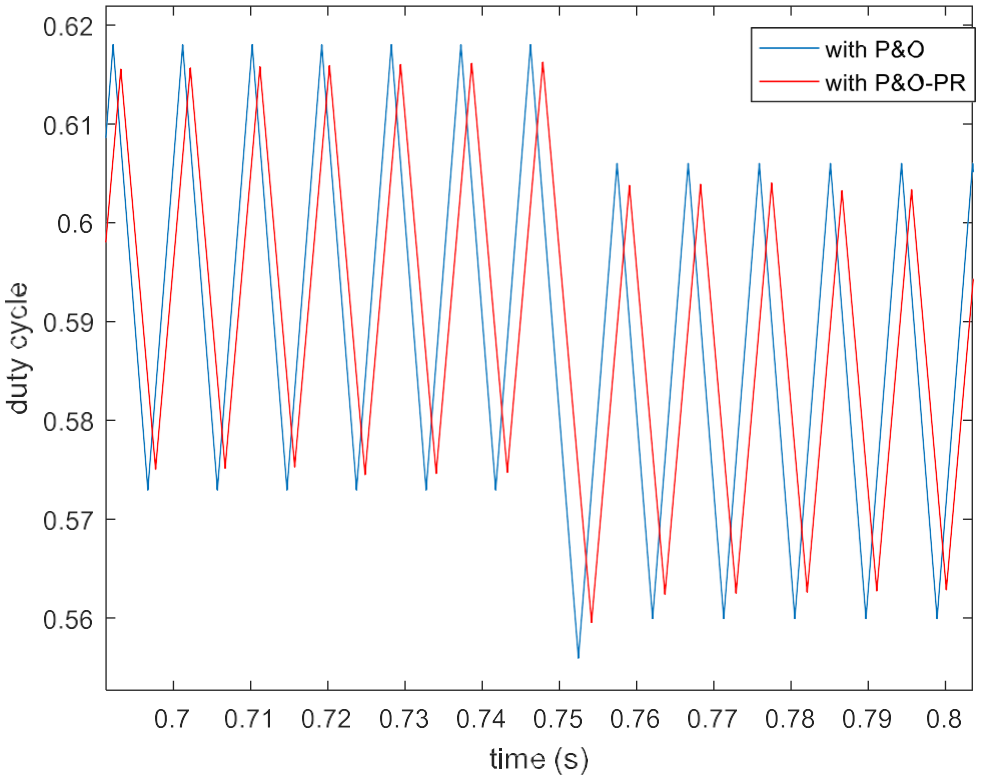


Fig III.14. Zoom at the duty cycle of PV module with P&O and P&O_PR

Variable Temperature [288 303 318 298 308]

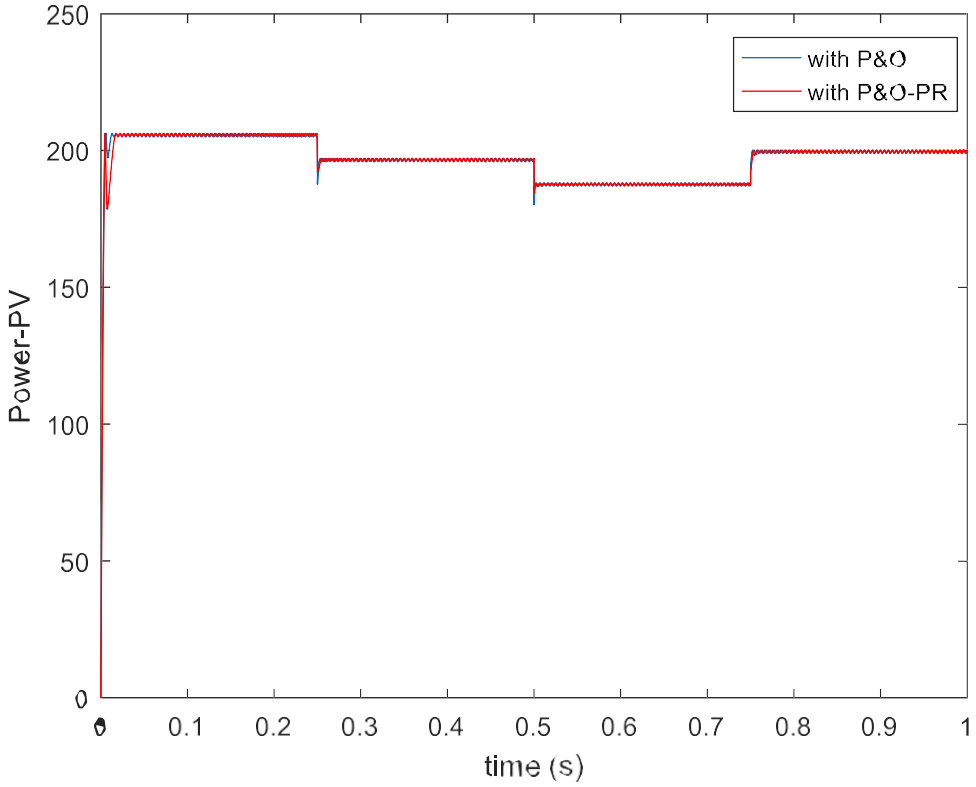


Fig III.15. The power of PV module with P&O and P&O_PR

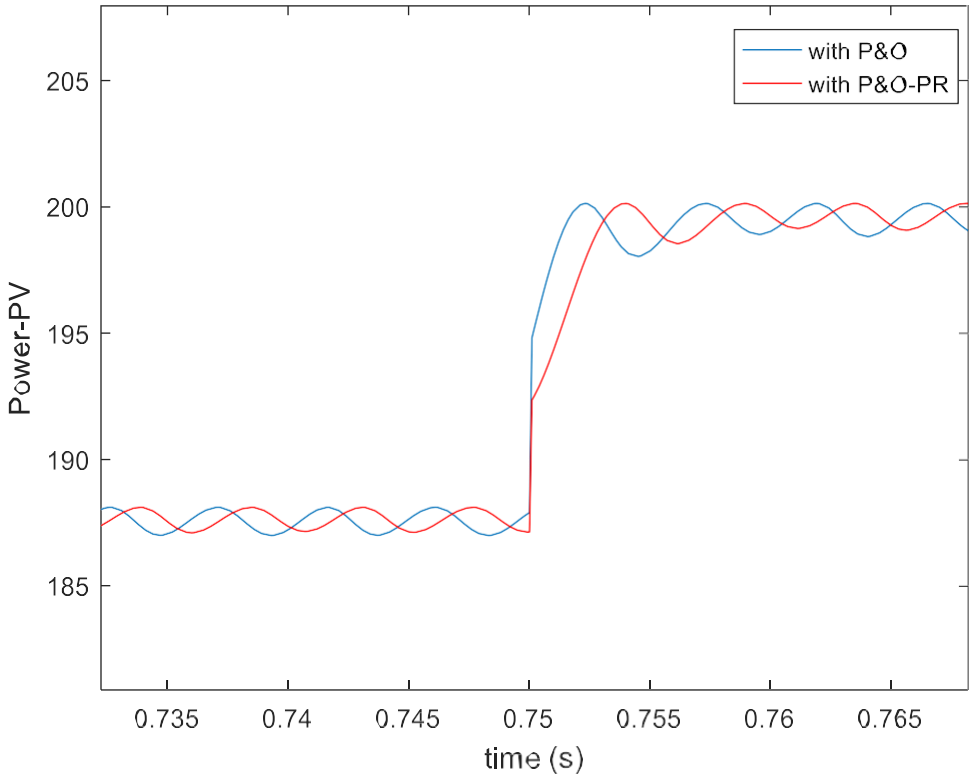


Fig III.16. Zoom at the power of PV module with P&O and P&O_PR

Variable insolation [500 700 1000 600 800]

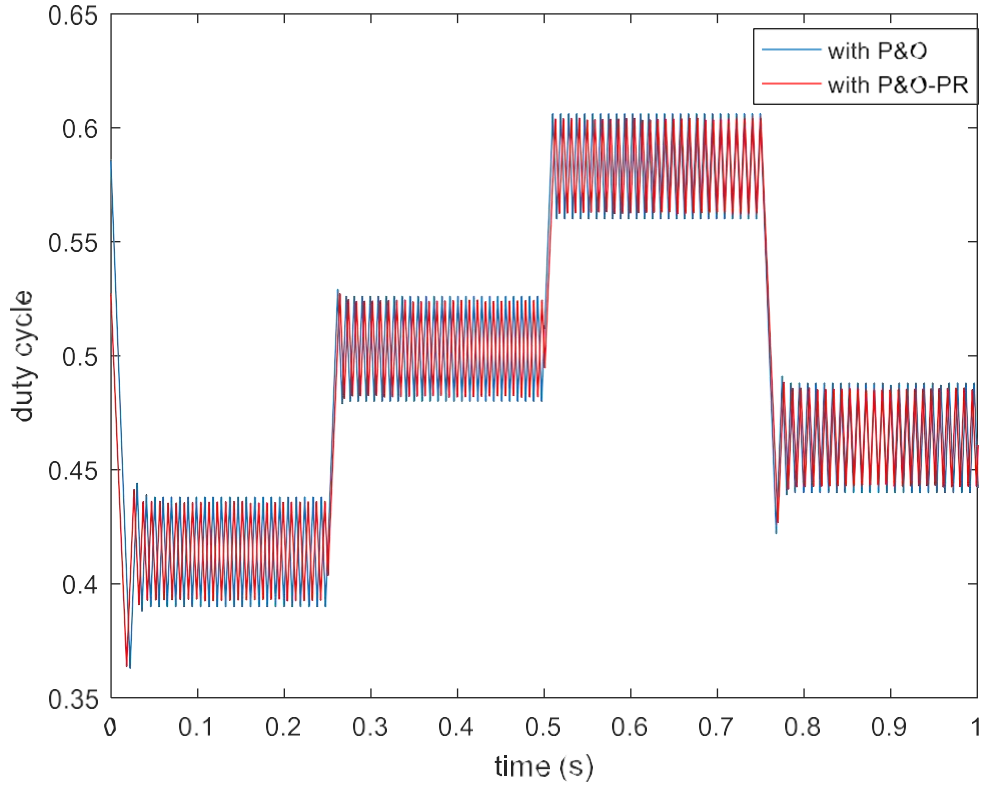


Fig III.17. The duty cycle of PV module with P&O and P&O_PR

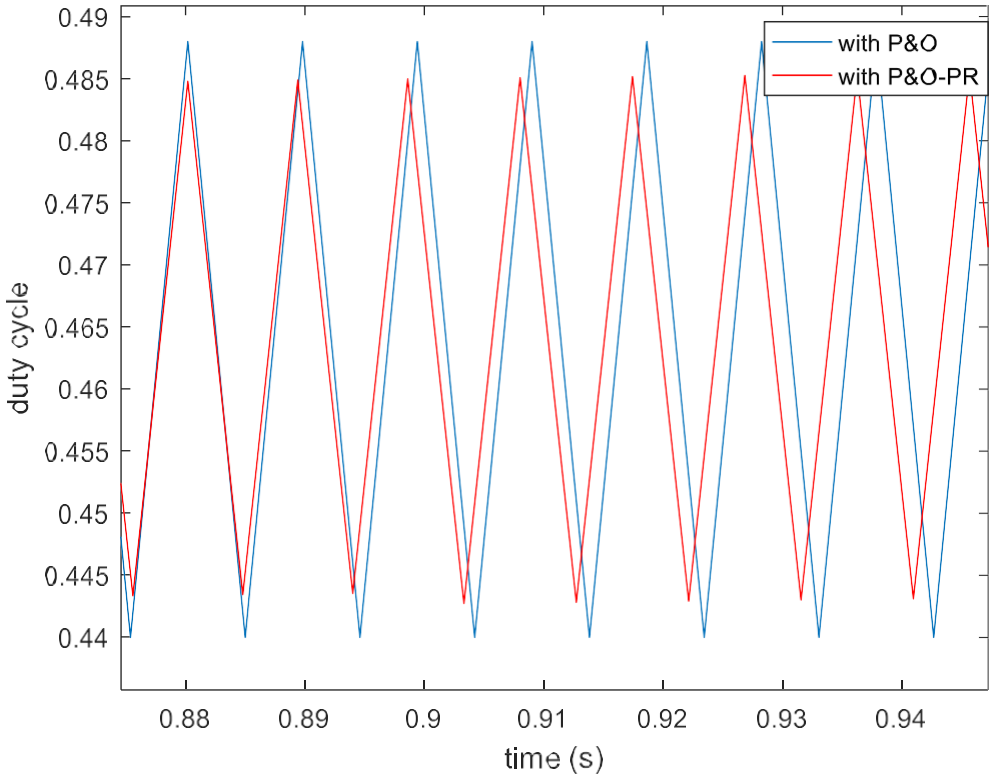


Fig III.18. Zoom at the duty cycle of PV module with P&O and P&O_PR

Variable insolation [500 700 1000 600 800]

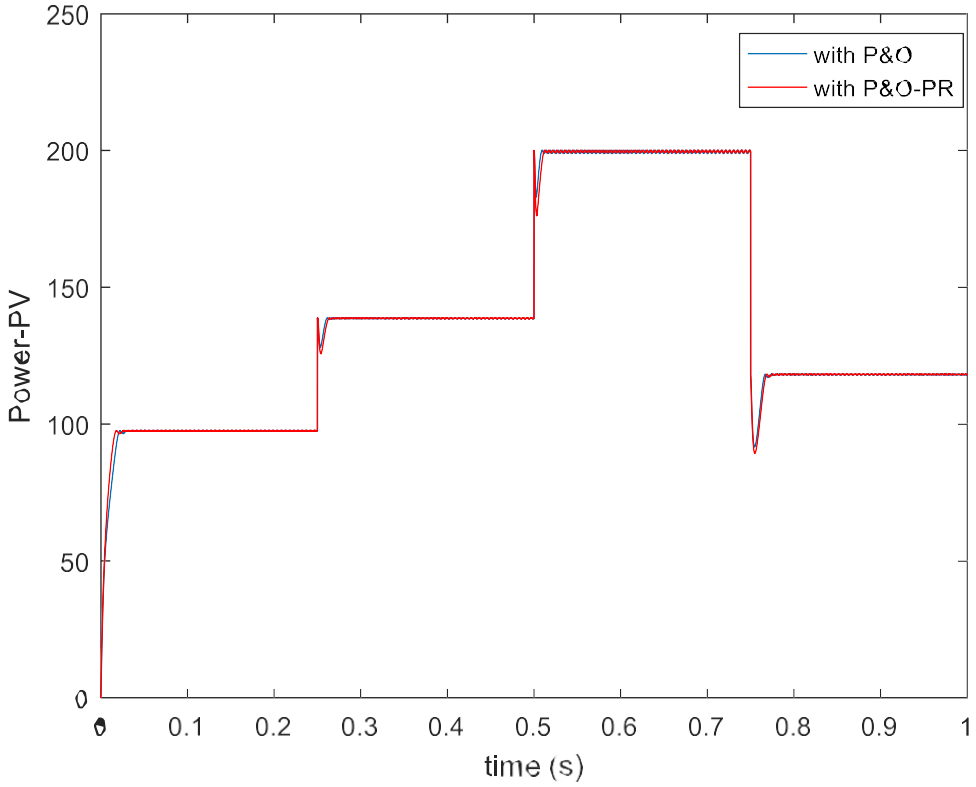


Fig III.19. The Power of PV module with P&O and P&O_PR

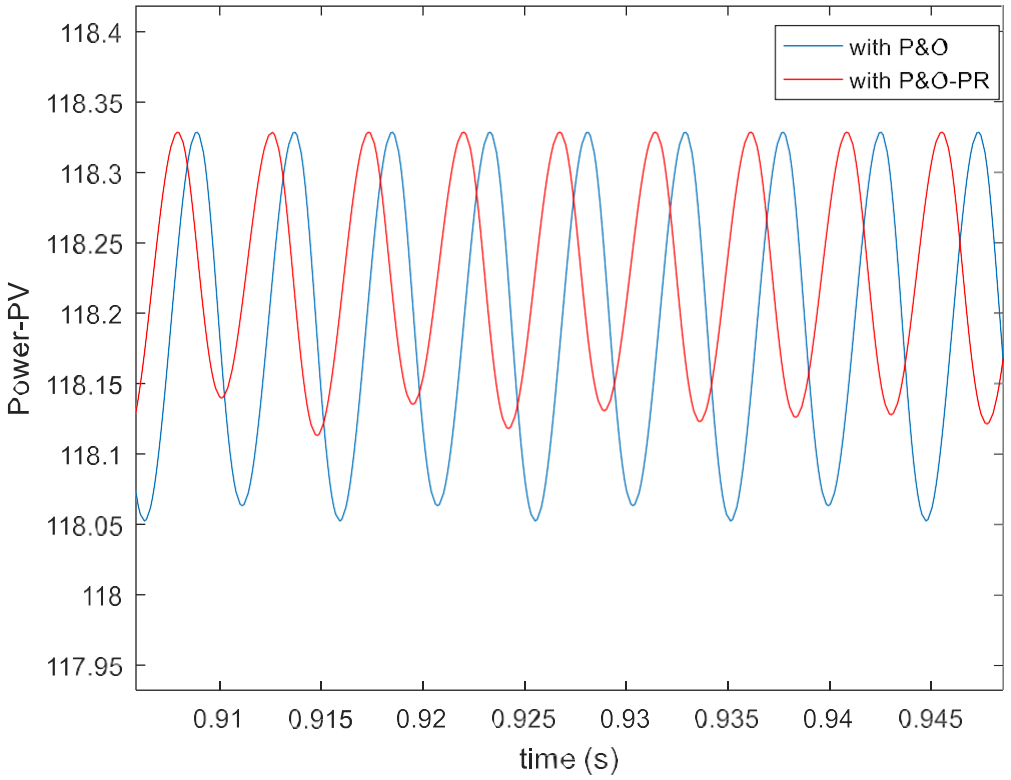


Fig III.20. Zoom at the Power of PV module with P&O and P&O_PR

III.7. Results Discussion

This section presents and analyzes the simulation results of a photovoltaic (PV) voltage regulation system that integrates a Proportional Resonant (PR) controller with the classical Perturb and Observe (P&O) algorithm. The objective is to evaluate the impact of the PR controller on improving dynamic performance, output stability, and energy efficiency under realistic conditions.

7.1 Output Power and Energy Efficiency

Figure III (7,15,19) illustrate the output power of the PV system for both control strategies. When using the classical P&O method alone, the power exhibits noticeable oscillations around the Maximum Power Point (MPP), which are inherent to the perturbation-based nature of the algorithm. In contrast, when the PR controller is integrated, these oscillations are significantly reduced. The power output reaches the MPP more quickly and maintains a more stable profile over time.

Quantitatively, the **efficiency criterion (Ef)**, defined as the ratio between the extracted power and the theoretical maximum power, shows an improvement from **Ef = 99.4778%** (P&O alone) to **Ef = 99.5547%** (P&O + PR). This highlights the effectiveness of the PR controller in refining the dynamic behavior of the voltage regulation loop and reducing energy losses due to poor voltage tracking.

7.2 Duty Cycle Behavior

Figure III (5,13,17) compare the duty cycle control signal over time. Under the classical P&O approach, the duty cycle exhibits continuous oscillations as the algorithm perturbs the operating point. These fluctuations can lead to increased switching losses and stress on the power electronic components.

With the addition of the PR controller, the duty cycle signal becomes smoother and more consistent. This is due to the enhanced tracking capability of the PR control, which quickly aligns the PV voltage with the desired reference value provided by the P&O. As a result, the converter operates more efficiently, with less control effort and reduced high-frequency variation in the control signal.

7.3 PV Voltage and Current Regulation

Figures III.9 and III.11 present the PV module voltage and current waveforms, respectively. In the case of the classical P&O, the voltage oscillates around the reference, especially under fast-changing irradiance or load conditions. This leads to current fluctuations and suboptimal operation.

The integration of the PR controller leads to significantly improved voltage tracking, with the PV voltage tightly following the reference. The current drawn from the module is also more stable, improving the reliability and thermal behavior of the system. The resonant nature of the PR controller helps in attenuating the low-frequency oscillations typically induced by P&O perturbations.

7.4 Control Signal Energy Consumption

Beyond output performance, it is important to assess the **energy consumption of the control signal**, which can affect the long-term efficiency and wear of the switching devices. We define this criterion as the time integral of the squared control effort (e.g., ∫u(t)2dt\int u(t)^2 dt) over a given time window.

The results show a **notable reduction** in control energy when the PR controller is used. This is attributed to the frequency-selective behavior of the PR controller, which applies high gain only at the necessary frequency (e.g., 50 Hz), reducing unnecessary control action and avoiding broadband amplification of noise or disturbances.

Comparative Performance

Criterion	**P&O Only**	**P&O + PR Controller**
Output Power Stability	Moderate (oscillations)	High (stable near MPP)
Efficiency (Ef)	99.4778%	99.5547
Duty Cycle Signal	Highly oscillatory	Smooth and consistent
Voltage Tracking	Delayed, oscillatory	Fast and accurate
Current Fluctuation	Significant	Reduced
Control Signal Energy Consumption	5828.4	5800.1

Table III.2: Comparative Performance

The integration of a Proportional Resonant controller into the voltage regulation loop of a PV system significantly enhances the performance of the conventional P&O MPPT algorithm. It improves stability, increases efficiency, reduces control effort, and minimizes oscillations in both electrical and control variables. These enhancements are particularly beneficial in real-world PV applications where the operating conditions are dynamic and high performance is critical.

III.8. Conclusion

This chapter has presented the design, implementation, and evaluation of a **Proportional Resonant (PR) controller** integrated with the classical **Perturb and Observe (P&O)** algorithm for improved voltage regulation in photovoltaic (PV) systems. Through comprehensive simulation studies, the proposed hybrid control strategy demonstrated clear advantages over the standalone P&O method, especially in terms of dynamic response, stability, and energy efficiency.

The results revealed that integrating the PR controller significantly **reduced oscillations** in the output power near the Maximum Power Point (MPP), leading to faster convergence and a more stable operating point. This directly contributed to an improvement in energy extraction efficiency, as confirmed by an increase in the efficiency criterion from **99.4778%** (P&O only) to **99.5547 %** (P&O + PR).

Furthermore, the **duty cycle signal** became smoother and more consistent under the hybrid approach, reducing switching losses and extending the lifespan of power electronic components. **Voltage tracking accuracy** was also significantly improved, with the PV voltage closely following its reference, resulting in reduced current fluctuations and enhanced system reliability under variable environmental conditions.

Additionally, the **energy consumed by the control signal**—quantified through the squared control effort—was notably lower when using the PR-enhanced approach, demonstrating a more efficient and selective control action.

Overall, this chapter confirms that the **PR controller complements the P&O algorithm** by addressing its main shortcomings, notably the oscillatory behavior and delayed response. The combined strategy delivers a **robust, high-performance MPPT and voltage regulation solution**, making it particularly well-suited for real-world PV applications where environmental conditions are dynamic and system efficiency is paramount.

General Conclusion

General Conclusion

In response to the growing global emphasis on renewable energy, this thesis has focused on improving the efficiency and dynamic performance of photovoltaic (PV) systems, particularly in the context of maximum power point tracking (MPPT) and voltage regulation. While the classical Perturb and Observe (P&O) algorithm remains one of the most widely used MPPT techniques due to its simplicity and ease of implementation, its performance is often hindered by persistent oscillations around the Maximum Power Point (MPP), slow transient response, and sensitivity to environmental disturbances.

To address these limitations, this research proposed the integration of a **Proportional Resonant (PR)** controller into the voltage regulation loop of a PV system operating under a P&O-based MPPT strategy. The proposed control architecture was thoroughly studied and validated through simulation, aiming to enhance system stability, reduce energy losses, and minimize the control effort required for accurate MPP tracking.

The thesis was structured into three main chapters. The first chapter presented a detailed mathematical model of the PV module, accounting for the influence of temperature and irradiance on the electrical characteristics of solar cells. This model served as a foundation for simulating real-world PV behavior.

In the second chapter, the P&O MPPT algorithm was implemented in both its direct and indirect control forms. The performance of the algorithm was evaluated under varying irradiance conditions, and its limitations in terms of oscillatory behavior and power tracking efficiency were clearly demonstrated.

The third and most significant chapter introduced the design and implementation of the PR controller, which was integrated into the PV system's voltage regulation loop. This novel approach was compared with the classical P&O method through a comprehensive set of simulations.

The **results discussion** highlighted several key improvements achieved by the proposed PR-enhanced system:

- **Output power** stability was greatly improved, with reduced oscillations and faster convergence to the MPP.

General Conclusion

- **Energy efficiency** (Ef) increased from **99.4778%** using P&O alone to **99.5547%** with the integrated PR controller.
- The **duty cycle signal** exhibited significantly smoother behavior, reducing converter stress and switching losses.
- **Voltage and current waveforms** were more stable and accurate, particularly under variable irradiance, demonstrating improved tracking and thermal performance.
- The **energy consumption of the control signal**, evaluated through the integral of squared control effort, decreased from **5828.4** to **5800.1**, confirming a more efficient use of control resources.

Collectively, these outcomes affirm the effectiveness of integrating a Proportional Resonant controller into PV systems to overcome the inherent limitations of the classical P&O method. This control strategy not only enhances tracking accuracy and stability but also improves energy efficiency and system longevity.

In conclusion, the approach presented in this thesis offers a viable and robust solution for real-world photovoltaic applications where fast dynamics, low energy loss, and stable operation are critical. The findings pave the way for future work involving experimental validation, adaptive PR tuning techniques, and real-time embedded system implementation to further optimize PV energy systems.

Bibliography

Bibliography

[1]: L. Zaghba1,A. Borni2, A. Bouchakour3, «Buck-boost converter system modelling and incremental inductance algorithm for photovoltaic system via Matlab/Simulink », Revue des Energies Renouvelables SIENR'14 Ghardaïa (2014) 63 – 70 .

[2]: Y. Koca1 ,Y. Aslan2, A. Yonetken3, « Boost Converter Design and Analysis for Photovoltaic Systems », 4th Inte . Conf. Eng ,(ICETAS) April 24-28 2019 Kiev Ukraine .

[3]: P. Kapadeeya1 , Prof R.P.Sukhadia2 , « MODELLING AND SIMULATION OF BOOST CONVERTER FOR SOLAR PV SYSTEM », Inte. Journal For Technological Research In Engineering Volume 3, Issue 7, March-2016 , ISSN (Online): 2347 – 4718 .

[4]: Z. Bala Duranay1, H. Guldemir2, « Voltage Controlled Boost Converter-Inverter System for Photovoltaic Applications », Turkish Journal of Science & Technology 15(2), 85- 92, 2020.

[5]: Rania G. Mohamed a1 , Hany M. Hasanien 2 , M.A. Ebrahim3, « Global MPPT controllers for enhancing dynamic performance of photovoltaic systems under partial shading condition », e-Prime-Advances in Electrical Engineering, Electronics and Energy ,9 ,(2024) .

[6]: Zerhouni, F. Z., Zegrar, M., & Stambouli, A. B. (2009). Connexion directe source d'énergie renouvelable verte non polluante photovoltaïque à une charge. Journal of Renewable Energies, 12(4), 585-595.

[7] : N DIAYE Papa Amadou, KAWTHER Achari. (2019) , "Production d'énergie électrique à partir d'un système photovoltaïque". (Thèse de Master, Université 8 Mai 1945 – Guelma).

[8] : SAIDI, Sirine. (2023). "Conception d'un régulateur solaire avec la commande MPPT" .(Thèse de Master, Université 8 Mai 1945 – Guelma).

[9] : Zahzouh, Radhwane, Abdelkader Yacoub, and Abdelhadi Litim. (2021), "ÉTUDE ET SIMULATION DE LA COMMANDE MPPT BASÉE SUR L'APPROCHE P&O". (Thèse de Master, Université Salhi Ahmed -Naama).

[10] : Pastor, A. C. (2006). "Conception et réalisation de modules photovoltaïques électroniques " (Thèse de Doctorat, INSA de Toulouse).

Bibliography

[11] : Yamani, A., & Diba, C. A. (2020). " Réalisation et optimisation des régulateurs de charge solaire". (Thèse de Master, Université Ibn Khaldoun-Tiaret-).

[12] : DRAIDI, D. (2022). " Réalisation d'un chargeur de Batterie Basé sur La commande MPPT photovoltaïque ", (Thèse de Master, Université 8 Mai 1945 – Guelma).

[13] : Rachida Ghernoug , Maroua Sadallah , Nour El Houda Dhou. (2021-2022). " Commande MPPT par la logique floue pour les systèmes Photovoltaïques ". (Thèse de Master, Université Echahid Hamma Lakhdar d'El-Oued).

[14] : Nassim, B., & Smail, B. (2018). " Commande directe par la méthode Incrémental Conductance (Inc-Cond) d'un panneau photovoltaïque ". (Thèse de Doctorat, Université Mouloud Mammeri).

[15]: Christopher, I. W., & Ramesh, R. (2013). " Comparative study of P&O and InC MPPT algorithms ". American Journal of Engineering Research (AJER), 2(12), 402-408.

[16]: SALMAN, Salman, AI, Xin, et WU, Zhouyang. "Design of a P-&-O algorithm based MPPT charge controller for a stand-alone 200W PV system". Protection and control of modern power systems, 2018, vol. 3, no 1, p. 1-8.

[17]: Mohamed, S. A., & Abd El Sattar, M. (2019). "A comparative study of P&O and INC maximum power point tracking techniques for grid-connected PV systems." .SN Applied Sciences, 1(2), 174.

[18]: Zečević, Ž., & Rolevski, M. (2020). "Neural network approach to MPPT control and irradiance estimation." . Applied sciences, 10(15), 5051.

[19]: Aloulou, O. (2024). " Utilisation des réseaux de neurones artificiels pour l'optimisation de la commande mppt et la détection des défauts des panneaux solaires ". (Thèse de Doctorat, Université du Québec en Abitibi-Témiscamingue).

[20]: Mr. OUARI Mondher, Mr. ZINE Yakoub. (2020). "Étude des commandes MPPT d'un système Photovoltaïque". (Thèse de Master, École nationale Polytechnique).

[21]:Gaied Chortane, B. (2022). Amélioration de l'algorithme MPPT pour un système PV par l'intégration des nouvelles techniques basées sur l'intelligence artificielle (Thèse de Doctorat, École de technologie supérieure).

[22]: Figure by Abdelkader Mahmoudi, Abdelbaki Djouambi, Djamel Rahem. (Juin 2017). "Réalisation d'un convertisseur DC/DC dans une chaine de conversion d'énergie photovoltaïque".(Thèse de Master, Université Larbi Ben M'Hidi - Oum El Bouaghi)

Bibliography

[23]: Figure by Vipin Kumar, Sandip Ghosh, N. K. Swami Naidu, Shyam Kamal, R. K. Saket, S. K. Nagar. (2021). " A current sensor based adaptive step-size MPPT with SEPIC converter for photovoltaic systems". Article of IET Renewable Power Generation

[24]: Figure by Amit Kumar Sharma ,Rupendra Kumar Pachauri 2ORCID,Sushabhan Choudhury ,Ahmad Faiz Minai 3ORCID,Majed A. Alotaibi,*ORCID,Hasmat Malik ,*ORCID andFausto Pedro García Márquez ."Role of Metaheuristic Approaches for Implementation of Integrated MPPT-PV Systems: A Comprehensive . Article Mathematics 2023, 11(2), 269

[25]: Figure by Pallavi Verma. "ASYMMETRICAL FUZZY LOGIC CONTROL BASED MPPT ALGORITHM FOR STAND-ALONE PV SYSTEM UNDER PARTIALLY SHADED CONDITIONS ", Article in Scientia Iranica · February 2019

[26]: Figure by Ali Husnain , M.Tariq Iqbal . Article of "Dynamic Modeling of a Micro Solar Electric Vehicle for Pakistan using Simulink". June 2022

[27]: Figure by Mohamed Derbeli, Cristian Napole, Oscar Barambones, Jesus Sanchez, Isidro Calvo, &Pablo Fernández-Bustamante. "Maximum Power Point Tracking Techniques for Photovoltaic Panel: A Review and Experimental Applications". Article of Energies 2021, 14, 7806

[28] : Narayana, A. B., Raju, P. G., & Ramana, K. V. (2018). " Proportional Resonant Controller with Resonant Harmonic Compensators for Three-Phase Multilevel Inverter ". International Research Journal of Engineering and Technology (IRJET), 6, 812-816.

[29] : Pereira, L. F. A., & Bazanella, A. S. (2015). Tuning rules for proportional resonant controllers. IEEE Transactions on Control Systems Technology, 23(5), 2010-2017.

[30] : Heredero-Peris, D., Chillón-Antón, C., Sánchez-Sánchez, E., & Montesinos-Miracle, D. (2019). Fractional proportional-resonant current controllers for voltage source converters. Electric Power Systems Research, 168, 20-45.

[31] : Figure by Shahbaz Amin Khawaja, Sahib Khan, Abdul Qayoom Dahani. Article · April 2018 ." Comparative Analysis About The Study of Maximum Power Point Tracking Algorithms: A Review ".Sukkur IBA University
Sukkur, Pakistan

[32] : Figure by Ghayda' A. Matarneh, Mohamed R. Gomaa. November 2022 , "Investigating the Effect of Temperature on the Performance of Photovoltaic Cell".Article in Journal of Applied Mathematics and Computation , Al-Hussein Bin Talal University, Jordan

Bibliography

[33] : Figure by Ravinder Kumar, Hari Om Bansal, Dinesh Kumar. research article " Improving power quality and load profile using PV-Battery-SAPF system with metaheuristic tuning and its HIL validation " Feb 2020